2014

Comparative Analysis of Selected Model Species used in Intervertebral Disc Research

Lauren A. Monaco
Wilfrid Laurier University, mona0470@mylaurier.ca

Recommended Citation

Wilfrid Laurier University

Comparative Analysis of Selected Model Species used in
Human Intervertebral Disc Research

A thesis

By

Lauren Angelica Monaco

Under the supervision of

Dr. Diane Gregory
Dr. Stephanie DeWitte-Orr

In fulfillment of the thesis requirement for the degree of

Master of Science
in
Integrative Biology

Waterloo, Ontario, Canada, 2014

Comparison of Model Species for Intervertebral Disc Research

Abstract

Model species are commonly used in scientific research to allow researchers to collect

data in a more controlled and accessible manner. In intervertebral disc (IVD) research the some

of the most commonly used models are bovine (cow) tail, porcine (pig) lumbar, and ovine

(sheep) spines. This project aimed to compare biomechanical, anatomical, and histological

properties of the IVD of these model species, and to compare selected properties of model IVDs

to IVDs of humans from data obtained in the literature. The tensile properties of the intralamellar

region of single layers of the annulus fibrosus (AF) were tested by pulling the fibres within the

tissue perpendicularly to their orientation within the IVD. This was done using the Biotester

5000 (Cellscale, Waterloo, On) rake system. Geometric measurements of IVD and vertebral

height were measured from sagittal and frontal x-ray images and anterior-poster (A-P) and lateral

width measurements were taken using digital calipers. Height and width ratios were calculated.

Water content was determined by 24 hours of incubation at 65 °C and normalized to dry weight.

A histological comparison was conducted by comparing collagen, proteoglycan, and cell types of

the three animal models using three separate stains: hematoxylin and eosin, safranin-O/ fast

green, and a combination stain of Weigert's hematoxylin, alcian blue, and picrosirus red. A

percent deviation calculation was conducted to compare model species values to human values

for the elastic modulus, geometric ratios, and water content. In general, it was found that the

bovine and ovine IVDs differed the most from one another in tensile properties, where the bovine displayed the lowest strains and highest stresses (and was consequently the stiffest model) while the ovine displayed the opposite (and was consequently the most compliant model); the porcine displayed stress and strain values intermediate to the other models. All models had unique IVD: vertebral height ratios, where the bovine had the largest ratio (and thus largest IVD height) and the ovine had the lowest (and thus smallest IVD height). The porcine and ovine IVDs displayed similar A-P: lateral width ratios, and the bovine had a width ratio closer to 1.0, suggesting a more circular shape. Distribution of collagen and proteoglycans were similar between species however, the porcine and the ovine had the highest concentration of cells compared to the bovine, and the bovine had a larger section of collagen type I in the outer AF. Percent deviations from published human data revealed that each animal model deviated differently from these values: the elastic modulus of the ovine AF, the height ratio of the bovine, and the width ratio of the porcine deviated the least from human values in comparison to the other species. These findings suggest that, depending on the application, one model is more appropriate than others. Specifically, the bovine and porcine are most appropriate for full joint and full IVD applications due to their geometrical shape, while the ovine is most appropriate for isolated tissue mechanics. Overall, the bovine and the ovine IVD differed the most from one another in all properties measured, and the porcine was intermediate between the two models.

Acknowledgements

This project has been a fascinating and challenging experience and it could not have been completed without the following people:

I would like to thank my committee members, Dr. Mike Wilkie and Dr. Peter Tiidus, and my advisors, Dr. Stephanie DeWitte-Orr and Dr. Diane Gregory, for all their help in this project. A very special thank to Dr. Diane Gregory for her endless support, patience and encouragement. Diane, you have truly been an inspiration to me and made me feel like a real scientist! I am so fortunate and grateful to have had a wonderful and knowledgeable advisor like you.

Thank you to my classmates and friends, especially Sarah Poynter, Tyler Weinhardt, Krysteena Gadzala, Courtney Clayson, and David Gadzala, for keeping me sane and making me laugh when I needed it most. Courtney, you're my partner in science crime and the only person I am proud to be a crazy cat lady with. Thank you for your help, your writing circle edits, and your friendship! David, your endless support and ability to put up with my quirks (a.k.a. whining) has gotten me through all the tough stages of this program. You kept me going and always put a smile on my face.

Lastly, I would like to thank my parents and my sisters, Bianca and Giovanna… and Kiki, Amore, and Beans (surprise, surprise). Thank you for your love, support, advice, and food money. I love you all so much and I would not be where I am today without you.

Comparison of Model Species for Intervertebral Disc Research

Table of Contents

List of Tables

List of Figures

List of Abbreviations

Comparison of Model Species for Intervertebral Disc Research

Comparison of Model Species for Intervertebral Disc Research

List of Tables

Comparison of Model Species for Intervertebral Disc Research

List of Figures and Illustrations

Comparison of Model Species for Intervertebral Disc Research

List of Abbreviations

- A-P: Anterior-posterior
- AF: Annulus fibrosus
- CCL: Chondrocyte-like cell(s)
- ECM: Extracellular matrix
- FBL: Fibroblast-like cell(s)
- FSU: Functional spine unit
- GAG: Glycosaminoglycan
- IVD: Intervertebral disc
- NC: Notochordal cell(s)
- NP: Nucleus pulposus
- PBS: Phosphate buffered saline

Chapter 1:

Introduction

1.1. General Introduction

Animal models are frequently used in scientific research to conduct tests and experiments in controlled settings to infer human results. The use of animal models in spine and intervertebral disc (IVD) studies allows researchers to control for factors that may have an effect on the health of the spine, including age, weight, diet, and activity level that are otherwise difficult to control for in human populations. Further, animal models are more accessible, both logistically and ethically, and can allow for both *in vivo* and *ex vivo* observation. Commonly used models in spine research are from the bovine (cow) tail, porcine (pig) cervical, and ovine (sheep) lumbar (Figure 1) segments of the spine. These models allow researchers to conduct tests and experiments on the spine to better understand the biomechanical and biochemical properties of the healthy adult IVD. Furthermore, models are used to study the progression of IVD disorders on both a micro- and macroscopic level, and can help determine preventative and rehabilitative therapies.

1.2 General Anatomy

Two of the most important functions of the spine are to bear loads and to protect the spinal cord. The spine is designed to withstand forces from multiple directions and orientations from both internal and external sources. The forces acting upon the spine are derived mainly from
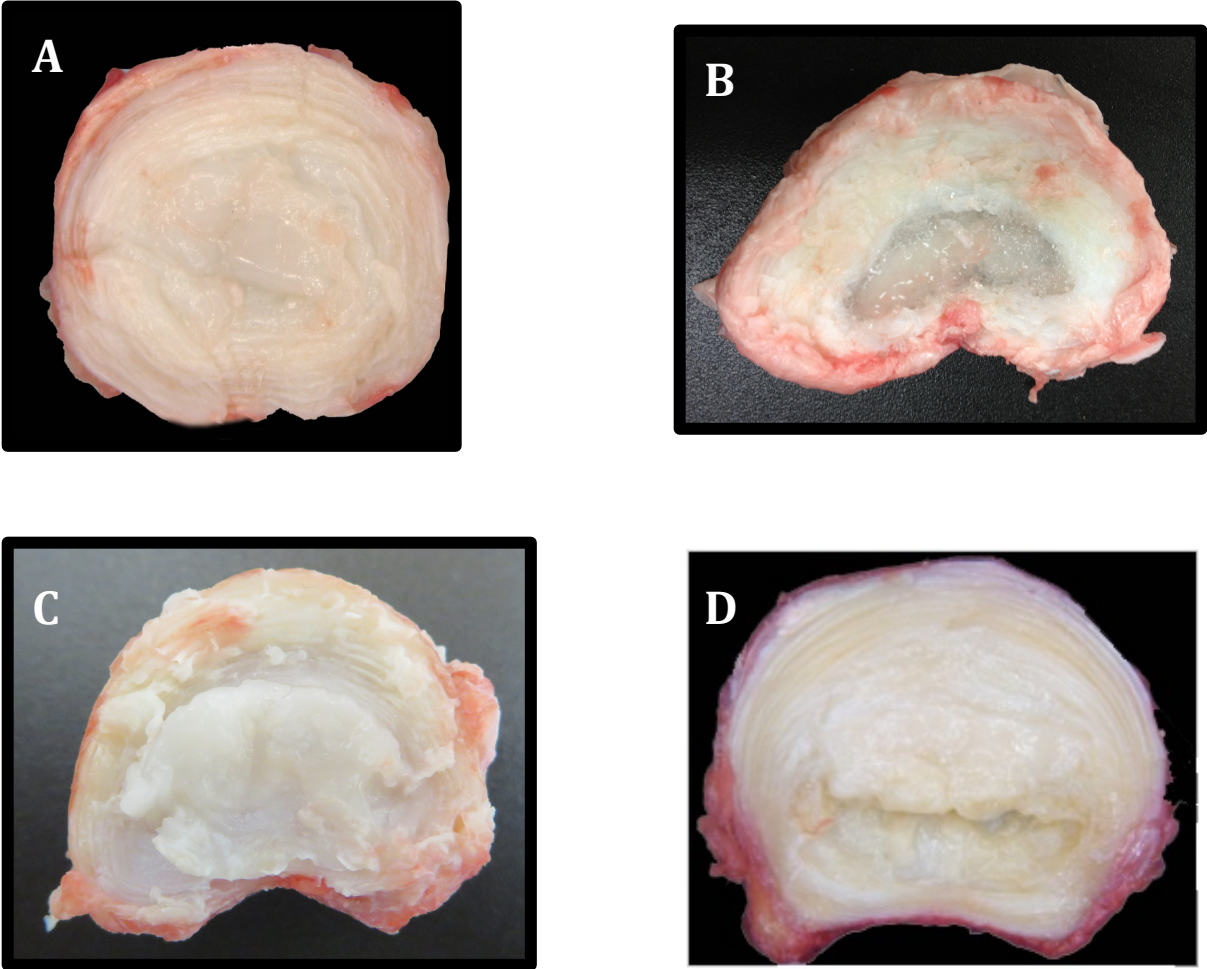
Figure 1. Representative intervertebral discs of bovine tail (A), porcine lumbar (B), and ovine lumbar (C) models, and human lumbar intervertebral disc (D).

contractions of the surrounding muscles, but are also caused by trunk and whole body movements (flexion-extension, bending, and torsion) as well as external forces. The spine utilizes specialized structures to compensate for such changes in the internal system of the body; one such structure is the IVD (Figure 1). The IVD is comprised of two main components: the annulus fibrosus (AF), which can be further broken down into the outer and inner layers, and the nucleus pulposus (NP) (Figure 2). As a whole, the IVD acts as a joint that allows flexibility to the otherwise rigid vertebrae of the spine, functions to support compressive loads from body weight and muscle tension, and anchors each vertebra to adjacent vertebrae (Urban et al., 2000). It is because of these imperative functions that any alterations modifying the internal integrity of the IVD can cause serious and debilitating consequences, such as IVD herniation, to the spine, including the surrounding muscles, vertebrae, and spinal cord.

1.2.1 Whole Intervertebral Disc Geometry

The 23 IVDs in the spine (6 cervical, 12 thoracic, 5 lumbar) comprise approximately 30% of the total vertebral column length (Panjabi & White, 1978) and are therefore great contributors to total body height. In a skeletally mature healthy young adult (20-40 years of age), the average IVD dimensions for height, lateral width, and anterior-posterior (A-P) width are 10.9 ± 0.8 mm, 55.4 ± 3.0 mm, and 37.7 ± 2.0 mm, respectively (Beckstein et al., 2008). These measurements emphasize a more oval, or limacon (McGill, 2007) shape of the human IVD, which can have
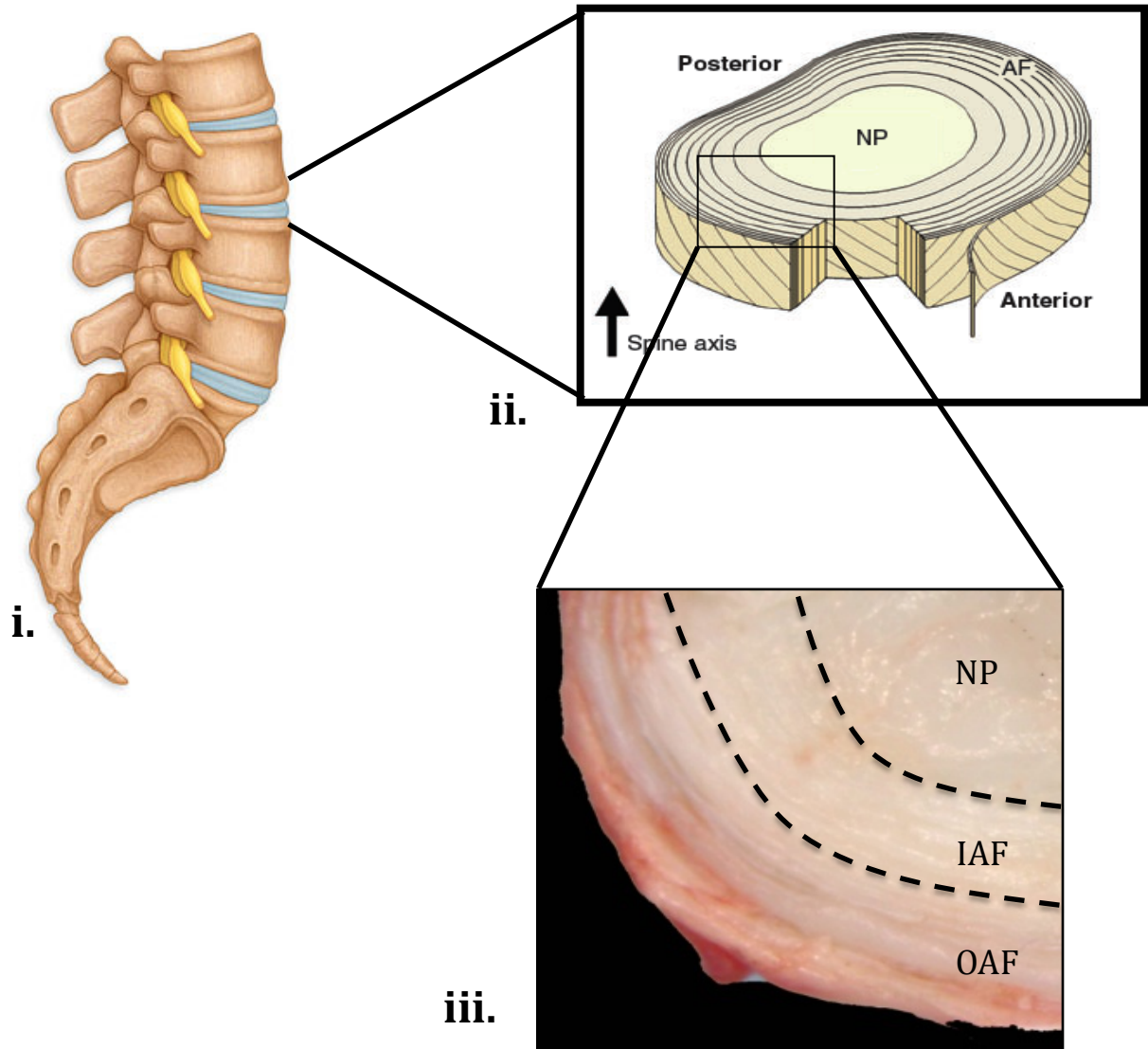
Figure 2. The anatomy of the intervertebral disc within the spine. Intervertebral disc in the lateral view (i) and whole intervertebral disc anatomy showing nucleus pulposus (NP) and annulus fibrosus (inner: IAF; outer: OAF) (ii). The intervertebral disc is further divided into outer annulus fibrosus, inner annulus fibrosus, and nucleus pulposus. The inner layers are those layers closest to the nucleus pulposus and the outer layers are those furthest from the nucleus pulposus.

Image (i) adapted from:

http://www.myissc.com/education/spine_health_encyclopedia/lumbar-spine---lateral-view.jpg .

Image (ii) adapted from:

http://dmm.biologists.org/content/4/1/31/F1.large.jpg

substantial effects on the distribution of forces and internal pressures within the IVD.

1.2.2 Hydration

Water content within the IVD is determined by the concentration of proteoglycans (especially aggrecan), due to their hydrophilic nature, and internal muscular pressure applied on the IVD (Urban et al, 2000). The amount of water differs radially within the disc, and is unique for each component of the IVD; the NP has the highest percentage of water and the outer AF has the lowest. On average, the water content of the NP, inner AF, and outer AF is 86 ± 4%, 82 ± 6%, and 74 ± 6%, respectively (Reid et al., 2002), where the inner regions function to withstand hydrostatic pressures more than the outer layers of the IVD (McNally & Adams, 1992) and this have a greater water content. Water plays a key role in supporting compressive loads acting upon the spine and body (Buckwalter et al., 1995), and comprises approximately 78 ± 3 % of the total extracellular matric (ECM) composition (Gower and Pedrini, 1969).

Water content changes drastically with age, especially within the NP. In a healthy IVD, water content in the NP is 82 ± 2%, whereas in aged individuals (60-80 years of age) water content is lost in the NP (75 ± 2%) (Antoniou et al., 1996). Additionally, a decrease in water content results in a decrease in IVD height. This decreases the IVDs ability to act hydrostatically and can lead to concentrated areas of stress and abnormal loading (Urban et al., 2000). Cracks and fissures may ultimately result within the IVD and further the progression of degeneration.

Water loss also increases the overall strain on the disc, as there is less water to cushion forces acting upon the spine (Stokes, 1987). Given that cadaveric spines are generally obtained from older individuals, it is important that any animal models used for IVD research have characteristics that more closely resemble that of a young healthy adult, rather than an older adult, to best represent this demographic that is affected by low back disorders.

1.2.3 Annulus Fibrosus Anatomy

The mesenchyme derived AF is comprised of highly organized fibrotic collagen layers (or lamellae) arranged concentrically around the NP. The number of lamellae within the IVD can range from a minimum of 15 layers posteriorly to a maximum of 25 layers laterally (Marchand & Ahmed, 1990) and are often thicker and more numerous anteriorly than posteriorly (Cassidy et al. 1989). The fibres within each lamellae run obliquely to the transverse plane of the spine at approximately 28° to 45°, where the angle increases from the outer AF to the inner AF (Holzapfel et al., 2005). The orientation of fibres in each neighbouring lamellae run perpendicularly to one another (Figure 3), which allows the IVD to withstand tension and compression in multiple directions and gives it its anisotropic property.
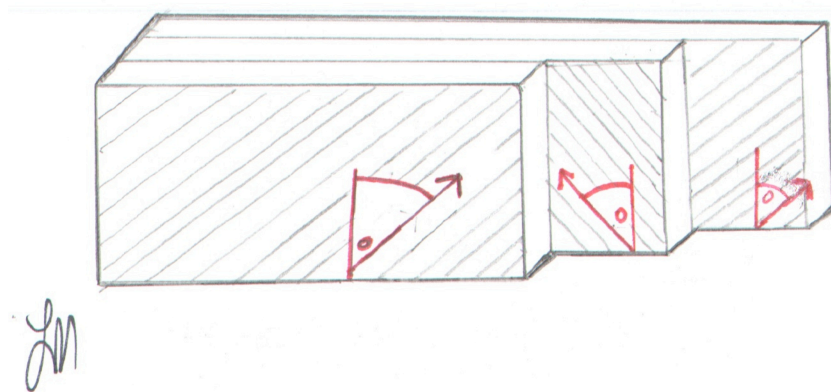
Figure 3. Annulus fibrosus layers fibre orientation shown for three adjacent layers. The arrows indicate the direction of the fibres. Arches represent the angle of the fibre with respect to axial plane. Note the alternating and perpendicular angles of the fibres in each adjacent layer.

The AF is composed of water (65-90%), collagen (50-70% dry weight), proteoglycans (10-20% dry weight), elastin (2%), and other non-collagenous proteins (Sun & Leong, 2004). The proportion of type I collagen decreases radially from 95% of the collagen present in the outer rim of the outer AF to ~0% in the NP (Berthet-Colomina et al., 1982); the concentration of type II collagen increases radially from the outer rim of the outer AF (~0%) to the NP (~95%) of the collagen types present (Berthet-Colomina et al., 1982). The remaining 5% composition of collagen within the AF and NP are collagen types III, V, VI, IX, and XI (McDevitt, 1988). The inner AF is known as the "transition zone" between the outer AF and NP and consequently contains a mixture of extra-cellular matrix (ECM) components of both outer AF and NP (Chou et al., 2006).

The region between individual lamellae in the AF is called the interlamellar matrix and functions to prevent delamination (separation) of the layers. The intralamellar matrix is the region between each individual collagen bundle within a single lamella, and functions to keep the collagen bundles tightly bound within the layer.

1.2.4 Nucleus Pulposus Anatomy

The NP is derived from the notochord during embryonic development, and is composed of a gelatinous core of unorganized structures. This core is contained circumferentially by the surrounding AF. The transition between the AF layers (especially the inner AF) and the NP is

often visually indistinctive but can be distinguished histologically by the proportion of ECM structures and cell types within each region.

The NP is rich in proteoglycans, water, and chondrocyte-like cells (CCL; Adams et al., 1977;) and contains collagen type II (Table 1). These ECM structure and cells aid in its ability to withstand and dissipate compressive forces acting upon the spine. The NP dissipates these forces by bulging outward and creating an internal hydrostatic pressure. This pushes the AF radially and puts tensile strain on the AF.

1.3 IVD Histology

1.3.1 Extracellular Matrix Proteins

The biomechanical properties of the IVD are not only dependent on the morphological structure of the IVD, but are also reflected in the extracellular matrix structure composition of each component. IVD degeneration disorders occur with age when water, ECM structures, and inter- and intralamellar matrices degrade within the IVD, leading to decreased IVD height, decreased ability to withstand forces, and ultimately leading to compromised integrity of the spinal column and surrounding ligaments and muscles (Urban and Roberts, 2003).

Table 1. Distribution of extracellular matric structures and cells within a healthy skeletally mature human intervertebral disc. Values taken from [1]Bron et al. (2009), [2]Cassidy et al. (1989), [3]Johnson & Roberts (2003), [4]Roberts & Urban (2011).

	Outer Annulus Fibrosus	**Inner Annulus Fibrosus**	**Nucleus Pulposus**
Water	65-90%[1]	65-90%[1]	77-88%[2,4]
Collagen Type	50-70%[1]; Primarily type I (95%)[2], some type II may be present; transitions to type II towards inner annulus fibrosus	50-70%[1]; Primarily type II (95%)[2], type I also present; decrease of type I towards nucleus pulposus	4%[4]; Type II
Proteoglycans	10-20%[1]	10-20%[1]	14%[4]
Cell types	Fibroblast-like[3]	Chondrocyte-like[3]	Chondrocyte-like[3]

There are four main types of ECM structures found within the IVD: collagen (mainly collagen I and II), proteoglycans, non- collagenous proteins (elastin), and water. Table 1 describes the proportion of the ECM structures within the IVD by component.

Proteoglycans are produced by all cells, especially CCL, and are highly hydrophilic. They are responsible for increasing the water content of the IVD and play a critical role in the biomechanical and load bearing function by increasing swelling pressure (Smith et al., 2011). Proteoglycans function to recruit water to areas of the IVD that respond to compressive loads (NP and inner AF). Due to a sulfate group on the glycosaminoglycan side chain, proteoglycans are negatively charged. This causes them to attract cations (or counterions), causing a charge gradient in the matrix and, in turn, recruits water via osmotic forces (Oegama et al., 1993). Water binds to these glycosaminoglycan side chains and becomes immobile within the tissue. In a healthy mature IVD, proteoglycans make up 466 ± 205 µg/g, 377 ± 185 µg/g, and 161 ± 31.9 µg/g of the dry weight of the NP, inner AF, and outer AF, respectively (Beckstein et al., 2008). Proteoglycans are comprised of a core protein with multiple covalently bonded glycosaminoglycan (GAG) side chains. Aggrecan is the most abundant proteoglycan and includes the chondroitin sulfate GAG side chain (Muir, 1995). Other GAGs include keratan sulfate and hyaluronan.

Two major types of collagen are found in the IVD: type I and type II. Type I collagen is found in tensile tissues throughout the body, such as in ligaments and tendons, and is known for its tensile strength (Lodish et al., 2000). Thus, it is mainly found in the outer AF, which functions to withstand tensile forces, and decreases in abundance radially inward from the outer AF to the NP (Figure 4). Type II collagen can be found in tissues under compression, such as articular cartilage, and function to withstand compressive forces, (Adams et al., 2006). It is therefore found in the more weight-bearing regions of the IVD: the inner AF and NP (Figure 4).

1.3.2 Cellular Composition

The IVD is a relatively acellular structure. It has a typical cell density of 5800 cells/ mm^3 which takes up approximately 25% of the total IVD volume (Maroudas, et al., 1975). There are three main types of cells found within the IVD: notochordal cells (NC), chondrocyte-like cells (CCL), and fibroblast-like cells (FBL) (Figure 5). The cell type present generally demarcates the areas of the IVD (i.e. outer AF, inner AF, NP) (Maroudas et al., 1975). Each cell type produces different ECM structures, which maintain the distinct biomechanical properties of the three regions of the IVD.

Some animals, such as non-chondrodystophoid dog breeds, porcines, and rabbits, retain their NC into adulthood, however, within the human IVD NC are generally only found in young spines and are lost in adulthood. NC are most abundant within the NP in skeletally immature

Type I	8	5	34	69	93	100
Type II	92	95	56	31	7	--
	1	2	3	4	5	6
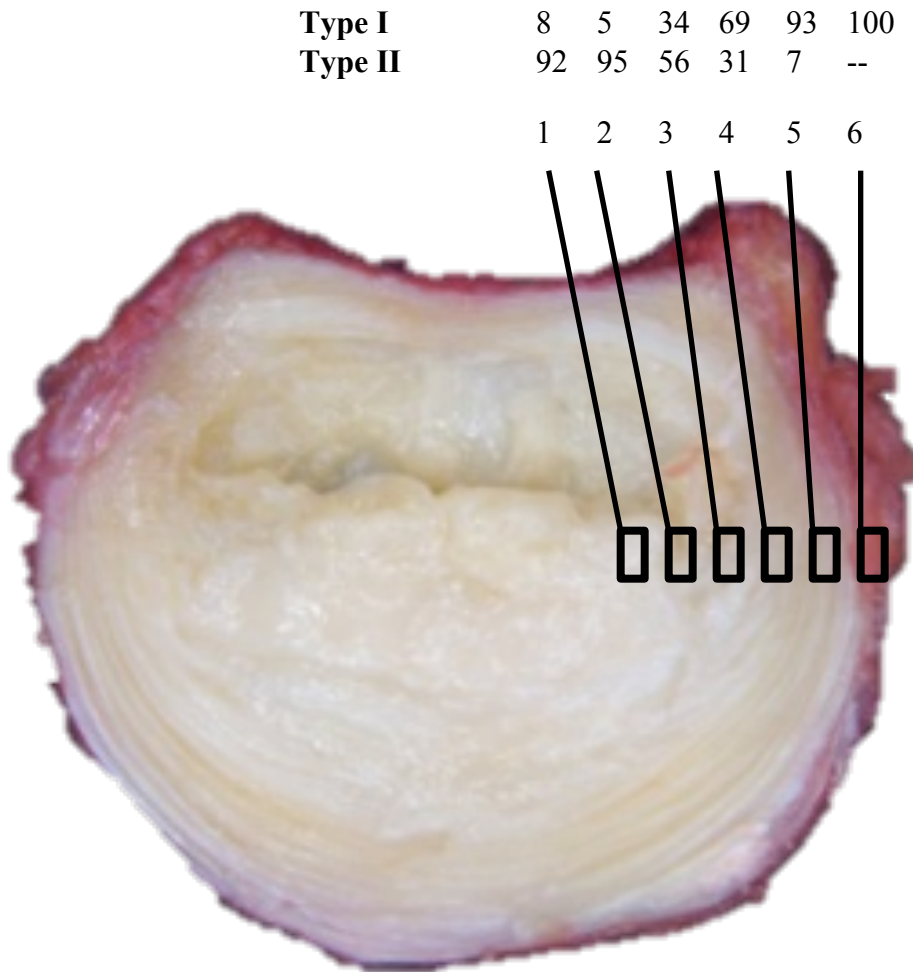
Figure 4. Distribution of collagens type I and II within the intervertebral disc, with respect to collagen type I and II. The gradual change in percentage of collagen type I and type II from the inner annulus fibrosus (1) to the outer annulus fibrosus (6). Values taken from Adams et al. (1997)
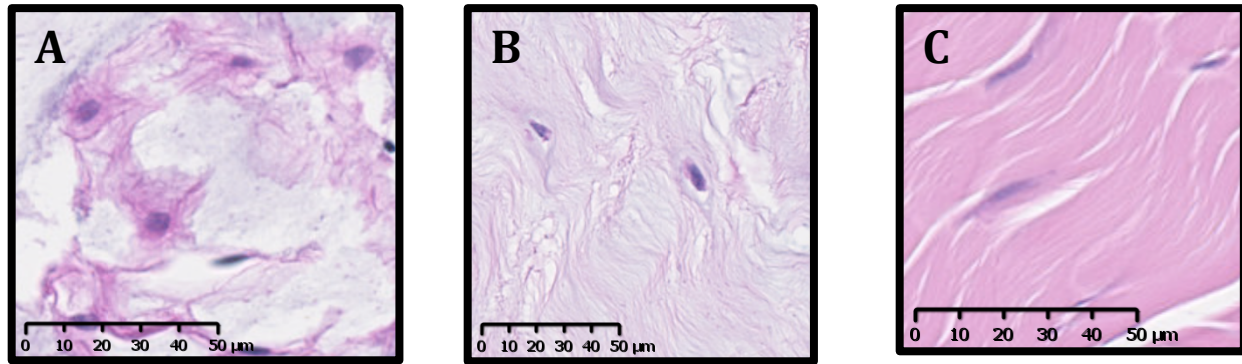
Figure 5. Fibroblast-like, chondrocyte-like and notochordal cell morphology. Morphology of notochordal (A), chondrocyte-like (B), and fibroblast-like (C) cells of the IVD from a porcine model. H & E, 40x, scale bar: 50 μm.

individuals under the age 10 years of age, after which they begin to be replaced by CCL (Trout et al., 1982).Young adult IVDs are not completely devoid of NC. These cells can be found within the IVD up until 30 years of age, however, the presence of NC has not been verified beyond this age (Trout et al., 1982). NC are large, round, and contain intracellular vacuole-like inclusion bodies (Hunter et al., 2004; Figure 5A.). They have higher nutritional demands and are less resistant to nutritional stress than their mature counterparts (Guehring et al., 2010). However, NC also maintain the hydration of the NP by increasing the production of ECM proteoglycans (Aguiar et al., 1999). The mechanisms which cause the turnover of NC to CCL are unclear, however, it has been hypothesized that increased mechanical forces, due to the maturation of the surrounding muscles and vertebrae, and a decreased nutrient supply, due to the maturation of the vertebral end plates and adjacent vertebrae, cause the replacement of NC by CCL (Guehring et al., 2009; Guehring et al, 2010). The retention of these cells through to adulthood can be seen in various species, including porcine and certain canine breeds, such as the greyhound (Ghosh et al., 1976). Additionally, it is hypothesized that the presence of NC protect the IVD from degenerative disorders (Geuhring et al., 2009), which can in part explain the lower frequency of low back disorders in children and youth.

CCL and FBL are similar to their namesakes, chondrocyte and fibroblast cells (respectively), in that they take on their similar morphology and characteristics (Chelberg et al.,

1995; Roberts et al., 2006), but are not chondrocyte, or fibroblast cells. CCL and FBL cells differ

from chondrocyte and fibroblastic cells in mechanical and chemical composition, as well as in

their interaction with other surrounding cells, where multiple junctions and connections can be

made between other CCL and FBL cells (Komuro, 1990). Junctions and connections between

CCL and FBL are used to correspond with interstitial cells and create an excitation-conducting

system that responds to mechanical stimuli (Kumoro, 1990). It is this one feature that

differentiates CCL and FBL from chondrocyte and fibroblast cells.

CCL are mainly found in the NP and inner AF (Errington et al., 1998). They are known

to synthesize a more collagenous ECM than NC by primarily producing type II collagen

(Chelberg et al., 1995), thus contributing to a less hydrated NP than in a skeletally immature

IVD. They also produce proteoglycans. Within the inner AF, CCL are round in morphology and

sparsely distributed (Figure 5B.) (Zhou et al., 2008). Within the NP, they bear small, cytoplasmic

processes and highly express ECM structures that contribute to the mechanical function of the

cytoskeleton of the cell (Trout et al., 1982; Zhou et al., 2008) by sensing mechanical strain

(Errington et al., 1998).

FBL cells are mainly found in the outer AF (Bruehlmann et al., 2002). They are

morphologically fusiform (Bruehlmann et al., 2002) (Figure 5C) and function to synthesize type

I collagen fibres within the IVD (Melrose et al., 2003) as well as proteoglycans. They have been

found to run parallel to the orientation of the collagen fibres within individual lamellae (Postacchini et al., 1984) and bear long processes (Errington et al., 1998). It has been hypothesized that in degenerated IVD, FBL cells replace CCL cells in the NP, resulting in an even more fibrotic and less liquid NP (Oegema, 1993).

1.4 Biomechanics of the Intervertebral Disc

The IVD is anisotropic such that it exhibits different mechanical properties when loaded in different directions. Although the outer AF, inner AF, and NP contain similar ECM and cellular structures, it is the proportion of them within a tissue that contributes to the biomechanics of each component. A stress-strain relationship, or a normalized force-displacement relationship (Figure 6), is used to quantify various material properties of tissues.

1.4.1 Stress-Strain Relationship

Stress is defined as the force per unit area that develops within a structure in response to externally applied loads, and strain is defined as deformation that occurs at a point in a structure under loading (Rodgers & Cavangh, 1984). In an engineering stress-strain relationship, stress is normalized by dividing the force acting on a tissue by the cross-sectional area of the tissue, with respect to the plane that the tissue is being deformed (Figure 7) and strain is normalized by dividing the total displacement of the tissue by the original length of the tissue (Figure 8).
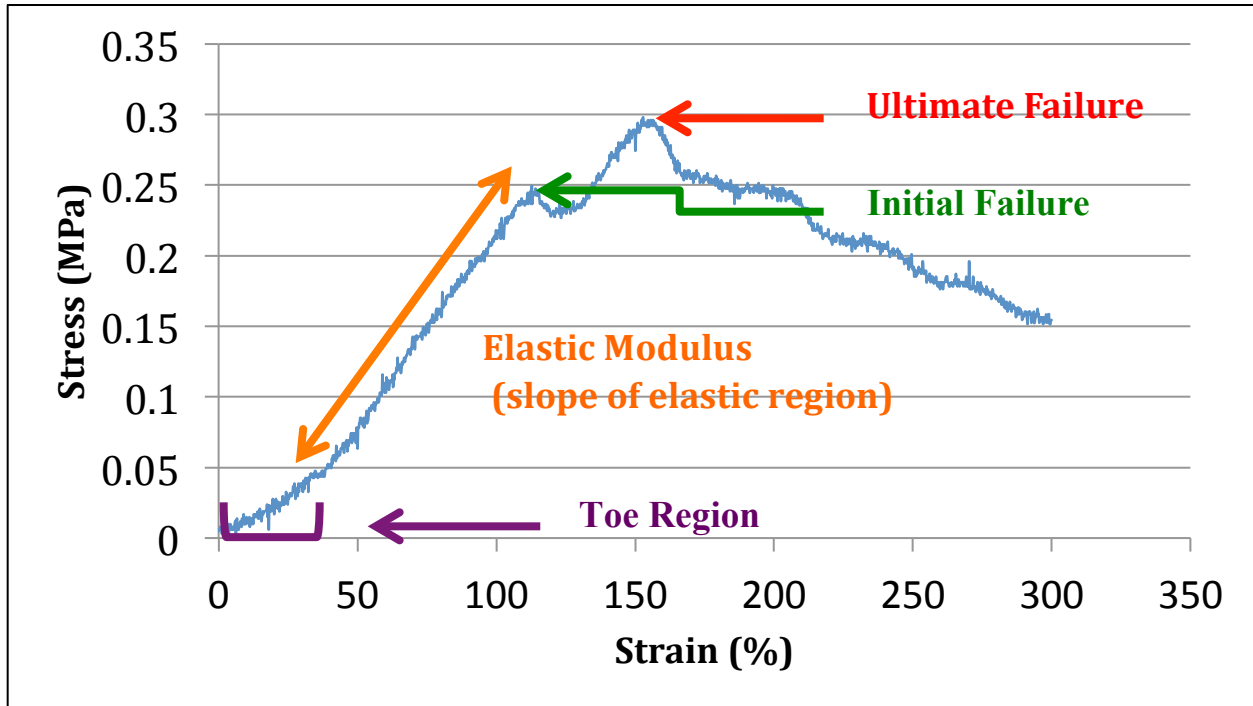
Figure 6. Stress-strain curve showing tensile property landmarks on graph. Sample Stress-Strain curve from a single layer of the annulus fibrosus from a porcine model indicating the toe-region (purple bracket), elastic region and elastic modulus (slope of the elastic region indicated by orange arrow), initial failure, and ultimate failure.
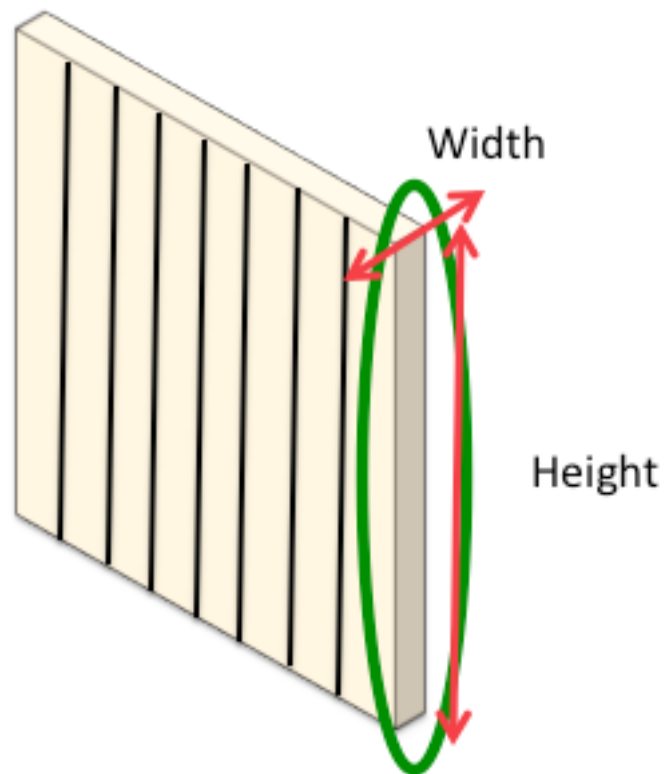
Figure 7. Measurement protocol for measuring cross-sectional area of single layer annulus fibrosus. Cross-sectional area of single layer tissue (encircled in green) used to calculate stress values. Height measurements were taken from LabJoy software output data and width measurements were taken using a laser displacement sensor (Keyence, Mississauga, Ontario).
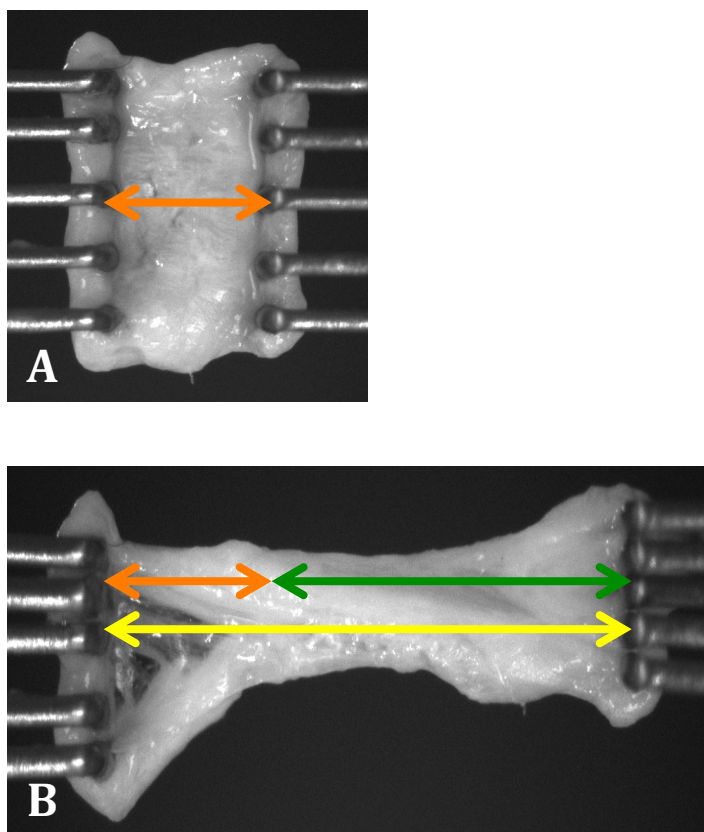
Figure 8. Single layer annulus fibrosus loaded in Biotester 5000 (Cellscale, Waterloo, Ontario) indicating original position and displacement of tissue during tensile testing. The original position of tissue (A; orange arrow) at the beginning of the testing protocol (displacement= 0), versus its position at the end of the protocol (B; yellow arrow), indicating the change in displacement of the tissue (B; green arrow). Images from bovine tail during tensile testing protocol.

Tension is described as the force caused when two forces acting in opposite directions pull an object apart (Rodgers and Cavangh, 1984). The tensile strength of the tissue describes the maximum tension that the tissue can withstand before ultimate failure of the tissue. Elastic modulus describes the stiffness of a tissue, and can be determined by the ratio of stress to strain at any point in the elastic region (Rodgers & Cavangh, 1984), or the slope of the elastic region (Figure 6). The initial failure describes the stress at which the tissue begins to form micro-tears but has not fully failed; this can be indicative of the forces that can lead to progression of IVD disorders, especially IVD herniation (Iatridis et al., 2005). Toe-region displacement (Figure 6) describes the amount of slack in the tissue. This region represents the "uncrimping" of collagen fibrils within the tissue and defines the length of the tissue before being exposed to constant tensile forces within the elastic region (Lundon, 2007).

1.4.2 Whole Intervertebral Disc Mechanics

The IVD is one of the main load bearing structures in the spine and thus has adaptations for cushioning and dispersion of compressive forces. This adaptation can be seen in the high proportion of proteoglycans and recruitment of water by ECM structures (mainly type II collagen and proteoglycans) within the NP as they are highly hydrophilic. The compressive forces act upon the NP and cause it to push outward and displace the lamellae, causing tensile stresses in the AF (Figure 9) (Nachemson, 1976). Furthermore, the pressure caused within the NP due to the
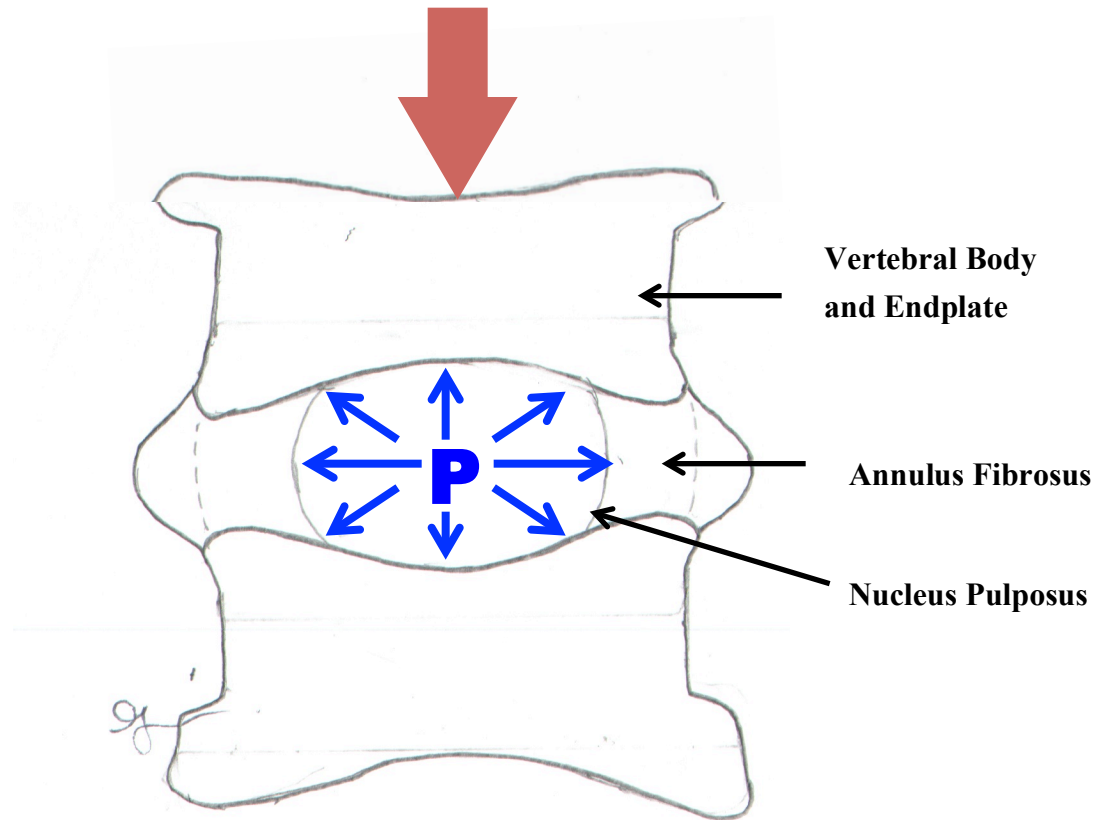
Figure 9. Anatomy of nucleus pulposus and annulus fibrosus of intervertebral disc under compressive forces. Internal pressure (P) of the nucleus pulposus due to compression forces (red arrow) from the vertebral endplate and vertebrae, which causes the annulus fibrosus to bulge outward, resulting in tensile stress with the annulus fibrosus.

compression of the vertebral endplate and vertebrae cause a radial transfer of forces and increase

the tensile stresses within the AF (Adams et al., 2006).

The forces acting on the areas of the IVD vary depending on the positioning of the body

and the spine (Skrzpiec et al., 2007). Regional variation of compression and tension in the

anterior and posterior sections of the IVD dramatically change within the IVD during spinal

bending, such as when an individual is sitting for an extending period of time or lifting heavy

objects. When an individual is flexed forward, the tensile forces are high within the posterior of

the IVD and can cause the AF to weaken in this area (Figure 10). In contrast, the compressive

forces on the anterior side of the IVD are greater and can result in the NP migrating posteriorly

through the weakened layers of the AF. This is one of the main mechanisms leading to IVD

herniation (Callaghan & McGill, 2001; Adams & Dolan, 1995).

1.4.3 Human Annulus Fibrosus Single Layer Mechanics

Very few studies have examined the mechanical properties of single layers of the AF, and

only two studies to date have tested single layers from actual human AF (Holzapfel et al, 2005;

Skaggs et al, 1994). Further, only one of these aforementioned studies has examined the tissue

properties both parallel and perpendicular to the orientation of the collagen fibres (Holzpafel et

al., 2005). Determining the tensile properties of single lamellae in both parallel and

Posterior   Tensile Force   **Anterior**
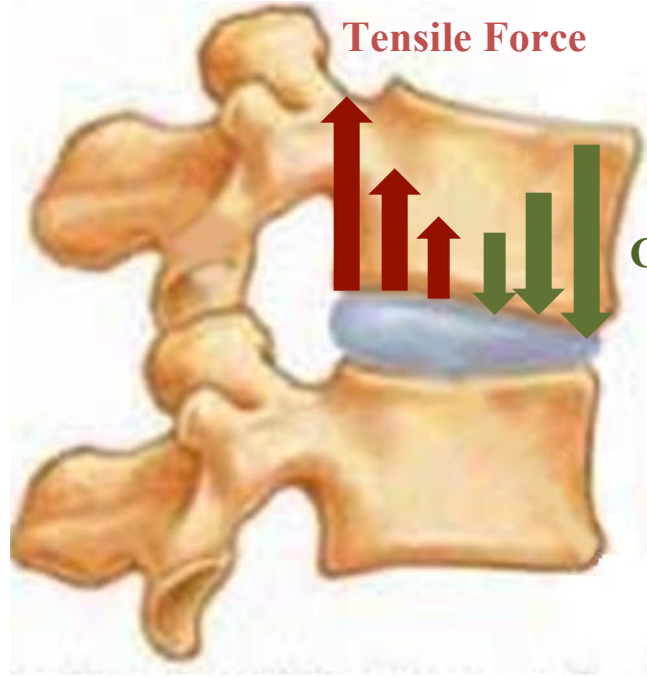
Compressive Force

Figure 10. Distribution of compressive and tensile forces on the intervertebral disc during forward bending. Note the higher degree of compressive forces on the anterior portion of the intervertebral disc and the higher degree of tensile forces on the posterior of the intervertebral disc.
Image adapted from: http://www.chiro.org/LINKS/Anatomy_101.shtml

perpendicular orientations can allow researchers to gain insight into the strength of the tissue, which is imperative to understand the development of IVD and low back disorders.

When pulled parallel to the collagen fibre orientation, Holzapfel et al. (2005) determined that human external lamellae (outer AF) are stiffer than internal lamellar (inner AF) and anterior tissues are stiffer than posterior (Table 2). This work was also found that the tensile strength of the outer layers was approximately 2-3 times higher than for the inner layers. This demonstrates the regional variation of properties within the IVD and supports the notion of an anisotropic IVD. All samples within this study, regardless of sample location within the IVD (i.e. A-P, or inner-outer), failed at stresses between 20 kPa and 150 kPa. Similar to Holzapfel, Skaggs et al. (1994) found that external lamellae had a higher elastic modulus than internal lamellae, and that lamellae in the anterior regions of the IVD had a greater stiffness than regions in the posterior-lateral (Table 2).

When pulled perpendicular to the collagen fibres, Holzapfel et al. (2005) found that single layers of the AF were much more compliant compared to tissues pulled in the parallel direction to their fibre orientation. Specifically, the elastic modulus perpendicular to the fibres was found to be 0.22 MPa (Table 3). No other tensile properties in this orientation were determined in this study.

Table 2. Tensile properties for single layers of the annulus fibrosus from human intervertebral disc samples pulled ***parallel*** to the collagen fibre orientation from samples taken from the anterior and posterior outer annulus fibrosus (OAF) and inner annulus fibrosus (IAF). Values taken from [1]Skaggs et al. (1994) and [2]Holzapfel et al. (2005).

Tensile Property	Location	Value	
Elastic Modulus (MPa)	Anterior OAF	136 (50)[1]	77.6 (20.0)[2]
	Posterior OAF	82 (43)[1]	64.8 (48.6)[2]
	Anterior IAF	76 (50)[1]	27.5 (12.8)[2]
	Posterior IAF	59 (41)[1]	31.2 (19.8)[2]

Table 3. Elastic modulus value for human single layer annulus fibrosus pulled ***perpendicular*** to collagen fibre orientation. Value from Holzapfel et al. (2005).

Tensile Property	Value (MPa)
Elastic Modulus (MPa)	0.22 (0.2)

1.5 Animal Models

Animals are used in research to model the reactions of the human body to particular disturbances in an individual's internal environment. Many spine and IVD studies have used animal models to understand the progression of spine disorders using numerous species, including porcine cervical (Gregory & Callaghan, 2012; Tampier et al, 2007; Callaghan and McGill, 2001), bovine tail (Yu et al., 2002), murine (rat and mouse) spines (Zhou et al., 2008), canine lumbar (Spitzbath, et al., 2012), rabbit spines (Gregory et al., 2014; Brown et al., 2011), ovine (sheep) lumbar (Veres et al., 2010), and cervine (deer) lumbar (Kumar et al., 2002) IVDs.

1.5.1   Geometry and Anatomy

Geometric measurements of the IVD can have a great influence on the biomechanics of the IVD and how it dissipates compressive and tensile forces. Table 4 displays the geometric measurements found from three different studies by Beckstein et al. (2008), Showalter et al. (2012), and O'Connell et al. (2007). In general O'Connell et al. (2007) found that the sheep IVD measurements deviated approximately 31% from the human IVDs, and the bovine tail deviated approximately 22% from the human IVDs, when whole IVDs were considered. No percent deviation was calculated for the porcine spine in this study, however, results from Beckstein et al. (2008) showed that the porcine lumbar IVD is consistently smaller for height, lateral width, and A-P width.

Table 4. Absolute values of height, lateral width, anterior-posterior width, and percent water content of human lumbar, bovine tail, porcine lumbar, and ovine lumbar intervertebral discs. Water content averaged across outer annulus fibrosus, inner annulus fibrosus, and nucleus pulposus; mean (standard deviation) reported. Values taken from Beckstein et al. (2008).

Species	Height (mm)	Lateral Width (mm)	Anterior-posterior Width (mm)	Water Content (%)
Human	10.91 (0.83)	55.38 (2.01)	37.67 (2.02)	77.67
Bovine	9.18 (0.65)	33.33 (2.51)	32.00 (3.58)	76.67
Porcine	5.46 (0.71)	37.13 (1.35)	25.26 (1.75)	70.33
Ovine	3.40 (0.46)	30.03 (1.20)	19.78 (1.43)	66

1.5.2   Histochemical Composition

The IVDs of certain animals may have a different response to similar forces due to an adaptation to a different environment than that of a human, such as diet or modes of locomotion. It is because of this that it is important to compare the biochemical composition of the tissue to determine the most appropriate model species for IVD study in humans, as the extracellular matrix structures and cell types alter the response of a tissue to a force.

In a study by Beckstein et al. (2008), it was found that the water content was significantly less than the human for the outer AF and inner AF of the porcine and ovine lumbar IVD (Table 5). The GAG dry weight of both the porcine and ovine lumbar differed significantly from the human IVD (Table 5). In general, it was found that the bovine tail IVD was a good model for human IVDs in terms of water content and GAG dry weight.

Bovine tail, ovine lumbar, and porcine lumbar IVD generally contain similar amounts of collagen to humans (Table 5). Significantly higher collagen contents were found within the NP of the bovine tail and the inner AF of the porcine lumbar when compared to humans (Showalter et al., 2012); no significant differences in collagen content were found for the ovine IVD.

Table 5. Absolute value for percent water content, proteoglycan (measured in sulfated glycosaminoglycans), and collagen content of the outer annulus fibrosus (OAF), inner annuls fibrosus (IAF), and nucleus pulposus (NP) of the human lumbar, bovine tail, ovine lumbar and porcine lumbar, as reported in [1]Beckstein et al. (2008) and [2]Showalter et al. (2012). (*) indicates significantly different values than the human. Collagen content data is normalized by dry weight. Mean (standard deviation) reported

Species	Age (years)	Region	Water Content (%)[1]	Sulfated Glycosaminoglycan Content (µg/mg dry weight)[1]	Collagen Content (µg/mg dry weight)[2]
Human	22-49	OAF	72 (3)	161 (31.9)	102.6 (18.9)
		IAF	80 (2)	377 (185)	47.9 (3.0)
		NP	81 (3)	466 (205)	15.6 (4.0)
Bovine	1.5-2.5	OAF	69 (3)	112 (26.6)	106.9 (23.4)
		IAF	78 (4)	394 (172)	70.7 (15.8)
		NP	83 (3)	548 (146)	43.4 (18)*
Ovine	3.5-5	OAF	57 (3)*	122 (36.2)	106.9 (18.4)
		IAF	66 (3)*	260 (55.5)*	66.8 (11.1)
		NP	75 (3)	547 (69.5)	19.2 (10.6)
Porcine	2	OAF	59 (2)*	71.8 (13.5)	122.4 (22.8)
		IAF	69 (2)*	150 (19.7)*	108.7 (6.4)*
		NP	83 (2)	379 (160)	5.8 (2.9)

1.5.3 Biomechanics of Model Intervertebral Discs

Very little is known about the biomechanical properties of single AF layers, which are the basic tensile units of the IVD (Skaggs, 1994). To the author's knowledge, only three studies have examined the mechanical properties of single layers of model species AF tissue (Pezowicz et al., 2005; Gregory & Callaghan, 2011; Gregory & Callaghan, 2012). Pezowicz et al. (2005) looked at the mechanics of single layers from bovine tail IVDs pulled parallel to their fibre orientation and found the initial failure stress and max failure stress to be 5.5 ± 1.8 MPa and 16.4 ± 8.0 MPa, respectively. When pulled perpendicular to the fibre orientation, the initial failure stress was found to reach 0.15 MPa (Table 2), however, no other tensile properties were tested.

Single lamellae tensile testing has also been conducted on herniated porcine cervical IVD pre- and post- disruption of the AF integrity through vibration and repetitive flexion (Gregory & Callaghan, 2011; Gregory & Callaghan, 2012). Table 6 summarizes the findings from these studies. In general, there was a significant difference found in failure strain of the single lamella tissues for those IVDs that had herniated after repetitive flexion versus those tissues that did not herniate after repetitive flexion, where lamellae failure occurred at higher strains than in unherniated IVDs. Additionally, there was a significantly different end of toe-region strain for lamellae that had been exposed to vibration than the control lamellae.

Table 6. Tensile testing results of single annulus fibrosus samples tested in the following conditions: "Control" – two hours of 1400N compression; "Vibrated" – two hours 5Hz compressive testing (1360-1540N); "Repetitive flexion" – two hours 1400N compressive and 1 Hz flex/ext; "Repetitive flexion with herniation" – two hours 1400N compressive and 1 Hz flex/ext resulting in intervertebral disc herniation; Gregory & Callaghan (2011)[a] and Gregory & Callaghan (2012)[b]. Results show mean (SD) values; (*) indicates significantly different results.

	End of Toe-Region Strain (%)	End of Toe-Region Stress (MPa)	Initial Failure Strain (%)	Initial Failure Stress (MPa)	Tensile Strength (MPa)	Failure Strain (%)
Control[b]	31 (15)*	0.33 (0.24)	57 (23)	1.09 (1.06)	1.44 (1.26)	117 (50)
Vibrated[b]	50 (33)*	0.59 (0.63)	81 (46)	1.36 (1.45)	1.62 (1.63)	115 (43)
Repetitive[a] Flexion	26.4 (39.7)	0.13 (0.09)	75.8 (37.9)	0.89 (0.48)	1.05 (0.58)	104.7 (47.0)*
Repetitive Flexion with Herniation[a]	16.3 (12.6)	0.13 (0.04)	43.5 (11.6)	1.14 (0.94)	1.34 (0.87)	60.4 (20.9)*

1.6 Intervertebral Disc Herniation and Low Back Disorders

Changes in the cellular and biochemical composition of the IVD can have a substantial effect on the overall biomechanics of the IVD and its ability to maintain stability within the spine. These changes can be caused by age (Trout et al., 1982; Boos et al., 2002), trauma (Tampier et al., 2007), and external environmental factors, such as repetitive vibration (Gregory & Callaghan, 2012), or repetitive movements, including forward flexion/extension of the spine (Callaghan and McGill, 2001). When several of these factors are combined, such as in a workplace setting, an individual may be at greater risk of developing a low back disorder (Pope et al., 2002). IVD disorders affect individuals worldwide, but are mainly observed in Western and employed populations (Katz, 2006). In general, there are more cases of IVD herniation in developed countries, especially in North America and Europe, which may be explained by the industrial lifestyle of these continents (Adams et al, 2006).

Faults, tears, weaknesses, and delamination within the intra- and interlamellar matrices can allow for the gelatinous contents of the NP to "push" through the AF layers, via radial fissures, when the IVDs are compressed. If the contents of the NP extrude through the layers of the AF, the IVD has become herniated. If the extruded NP comes into contact with the epidural space surrounding the spinal cord, cytokines are released from cell in the extruded content, and

an inflammatory response pathway results (Doita et al., 1996). The extruded NP then hardens

and impinges upon the closest nerve root (Figure 11.A).

IVD herniation is the major cause of nerve root pain, commonly known as sciatica

(Adams et al., 2006). The herniated fragment of the IVD impinges upon the nerve root and can

cause severe pain in the buttocks, back of the thighs, and lower back, in the form of recurrent

attacks (DePalma & Rothman, 1970), depending on what level the IVD has been herniated

(Figure 11.B).

IVD herniation is a common ailment among young to middle aged adults (Smith et al.,

2011; Adams et al., 2006). As individuals age, water and proteoglycan content decrease within

the IVD, especially within the NP (Gower & Pedrini, 1969). In aged persons the NP does not

have the fluidity to travel thorough the fissures and tears in the AF, leading to a decreased

incident of IVD herniation. Children tend to have a more liquid NP, however, children are not at

a great risk of herniation. This could be due to the high presence of NC cells, as they have been

hypothesized to contribute to IVD regeneration and prevention of damage (Guehring et al.,

2010). Therefore, the occurrence of IVD disorders, especially degeneration and herniation, has
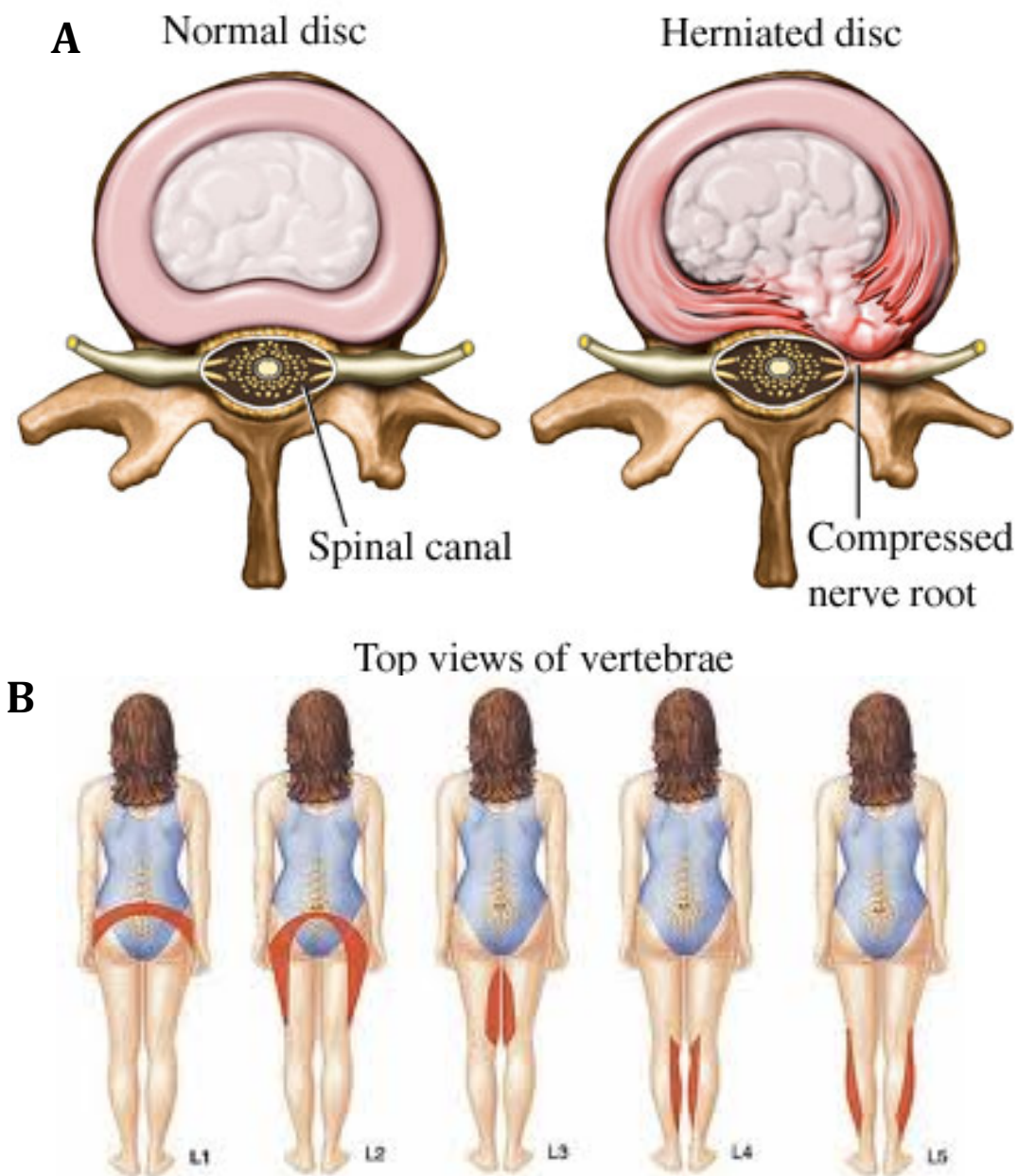
Figure 11. Anatomy of healthy and herniated intervertebral disc and resulting areas of pain on body after herniation of intervertebral disc at particular lumbar levels that affects nerve roots. (A) Comparison of a normal intervertebral disc to a herniated intervertebral disc; note the compression of nerve root by extruded nucleus pulposus in the herniated intervertebral disc on the right. (B) A herniated intervertebral disc can cause pain in the lower limbs in different regions depending on what level the intervertebral disc has herniated. L1-5 indicate lumbar intervertebral disc at levels 1-5.

Image (A) taken from http://physioworks.com.au/images/Injuries-Conditions/Bulging-Disc.jpg; image (B) taken from http://umm.edu/programs/spine/health/guides/lumbar-herniated-disc.

not been noted in individuals that are not skeletally mature. Additionally, children do not participate in activities as often as adults that may lead to forward flexion, such as lifting or sedentary work. Hence, IVD herniation is often seen in young to middle aged adults, where the fluidity of the NP, the relatively more damaged AF, and the increase incidence of physical activity that can cause herniation, leads to a combination of factors that increases the risk and occurrence of IVD herniation.

1.7 Purpose, Rationale, and Hypotheses

The purpose of this study is to conduct a cross species analysis of IVD of model species that are most commonly used in IVD research: bovine tail, porcine lumbar, and ovine lumbar. A secondary purpose is to determine if one single model is appropriate for IVD research or if each model is appropriate for specific spine applications. Specifically, this project seeks to compare the biomechanical, anatomical, geometrical, and histological properties of the IVD. Conducting a cross species comparison will determine if differences in properties exist between the models, and where these differences exist. Comparing the data from the model species with human data from previous literature can give insight to the most appropriate animal model for specific IVD research.

1.7.1 Specific Rationale for Biomechanical Analysis

The AF functions to withstand tensile forces caused by the hydrostatic pressure within

the NP due to the compression of the axial skeleton (Ghosh et al., 1976). The deterioration of the

intralamellar region of the AF can lead to the progression of low back disorders, particularly IVD

herniation. It is important to determine the biomechanical properties of this region in order to

better understand the magnitude and type of forces that the IVD can withstand and in turn

understand the progression of low back disorders. This project seeks to determine the tensile

properties (toe region stress/strain, initial failure stress/strain, ultimate failure stress/strain, and

elastic modulus) of the intralamellar of single layer tissues of the AF, by pulling the fibres

perpendicular to their orientation within the tissue. In doing so, the basic tensile structure (AF

single layer) of the IVD can be compared between models and an appropriate biomechanical

model can be determined for both whole disc and component research. Isolating the intralamellar

matrix has been successful in a few only studies (Gregory and Callaghan, 2011; Gregory and

Callaghan, 2012; Holzapfel et al., 2005; Pezowicz et al., 2005) and is an involved dissection to

obtain single lamellae tissue.

1.7.2 Specific Rationale for Anatomical and Hydration Analysis

Ratios of IVD: vertebral body heights can help infer force distribution patterns within the

IVD (and ultimately biomechanical differences), whereas width ratios (AP: lateral width) will

reveal approximate shape patterns. Ratios will allow for a normalized comparison of the models

and will eliminate any bias towards magnitude differences. Additionally, using both the height

and width ratios will allow for a better understand of whether a functional spine unit (FSU) can

properly emulate the forces seen within the human IVD.

Water content within the NP causes hydrostatic pressure within the IVD with

compression of the axial spine. In turn, the hydrostatic pressure within the NP exerts tensile

forces on the surrounding AF. Water content can be determined by many factors, including age,

ECM structures, and cell types. Therefore, determining water content will help reveal

information on the biomechanics of the IVD and the presence or absence of particular ECM

structures and cell types.

1.7.3 Rationale for Histological Analysis: Extracellular Matrix Structures and Cell Types

The presence or absence of cell types within the IVD and, ultimately, the composition of

the extracellular matrix composition, contributes to the biomechanical characteristics of the IVD.

The cells present in the IVD produce proteins, including proteoglycans and collagens, which aid

in the recruitment of water and function to withstand tensile and compressive forces. Comparing

the presence, absence, and relative abundance of cell types and extracellular matrix structures

within the IVD can allow for inferences to be made regarding the biomechanical function of a

model species' IVD.

1.7.4   Hypotheses

The overall general hypothesis was that the porcine and ovine models will be the most similar to one another because *in vivo* the IVDs are both located in the lumbar region of the spine, whereas *in vivo* the bovine IVD is located within the tail. Specifically, it was hypothesized that:

1. Models will exhibit different geometric properties and water content:

    a. Bovine tail will differ the most geometrically due to IVD location

    b. Porcine will have the highest water content due to a more liquid NP

2. Models will exhibit different biomechanical properties:

    a. Models that differ the most from one another geometrically (i.e. height and width ratios) will exhibit significantly different tensile properties

    b. Models with similar proportion and abundance of cell types and ECM structures will exhibit similar tensile properties

3. Models will exhibit different proportion of ECM proteins and cell types:

    a. The porcine NP will have a higher content of notochordal cells and proteoglycans due to a more liquid NP

4. Individual models will be appropriate to represent human IVDs depending on the application of the research

Chapter 2:

Materials and Methods

2.1 Biomechanical Protocol

2.1.1 Tissue Preparation

Frozen spine segments were cut into individual FSUs, and IVDs were randomly assigned for tensile testing protocol. Anterior and posterior samples were extracted from one IVD per spine from five different animals for each of the three species, for a total of 15 IVDs. IVDs were extracted from caudal levels 1-3 in bovine tails, and lumbar levels 1-4 in both porcine and ovine models (Figure 12). All spines were frozen after death and stored at -20°C until use.

Two anterior and two posterior single layer samples were dissected per IVD, for a total of 20 samples per species and 60 samples overall. However, due to testing system constraints, only 53 samples were further mechanically tested (Table 7).

Tissue samples were obtained while the disc was attached to adjacent vertebrae and while the tissue was frozen for ease of dissection. Each sample was tested promptly after extraction, at which time the tissues were full thawed, to prevent desiccation and fraying of collagen bundles. Both FSUs and individual samples were kept moist using phosphate buffered saline (PBS). Before testing and data collection, samples were viewed under an SP-SCD Trinocular Stereoscope (Leica, Wetzlar, Germany) to ensure that only a single layer was present in the sample.

Figure 12. Spine segments of bovine tail (above), porcine spine (middle), and ovine lumbar (bottom) indicating intervertebral disc levels used for testing.

Table 7. Distribution of sample size for single layer annulus fibrosus tissues used for biomechanical testing for bovine tail, porcine lumbar, and ovine lumbar.

Species	# Discs per spine	# Spines	Anterior	Posterior	Total
Bovine	1	5	10	7	17
Porcine	1	5	10	9	19
Ovine	1	5	10	7	17
					n= 53

Spines of the same species were collected from a single abattoir in the Kitchener-Waterloo or southern Ontario region, with the exception of ovine spines due to seasonal availability. This allowed for a reduced variability in diet, husbandry techniques, and age of slaughter within a species. Additionally, all animals were skeletally mature at time of slaughter. All tissues were pre-screened to determine if any degeneration or disease was present within the pre-mortem IVD, based on classifications seen in Adams et al. (1996).

2.1.2 Tensile Testing Protocol

Prior to tensile testing, AF layer width was determined using a laser displacement sensor (Keyence, Mississauga, Ontario), which measured the difference in the distance between the plate in which the tissue was placed and the laser, and the distance between tissue and the laser. The tissue was mounted into the BioTester5000 tensile testing machine (Cellscale, Waterloo, Ontario) (Figure 13A), and secured into place using five-prong tungsten rakes with an inter-rake distance of 0.7 mm. The tissue was positioned such that the orientation of the fibers within the layer ran perpendicular to the direction the fibers were being pulled (Figure 13B). Once loaded, the rakes were jogged out to a force of 10 mN, or when fibers within the tissue became taut. Tissues were preconditioned to 10% displacement at 1% displacement/second for three repetitions. Following preconditioning, tissues were pulled uniaxially until failure at a rate of 2% displacement/second for a total displacement of 300% original length. A 20 second recovery
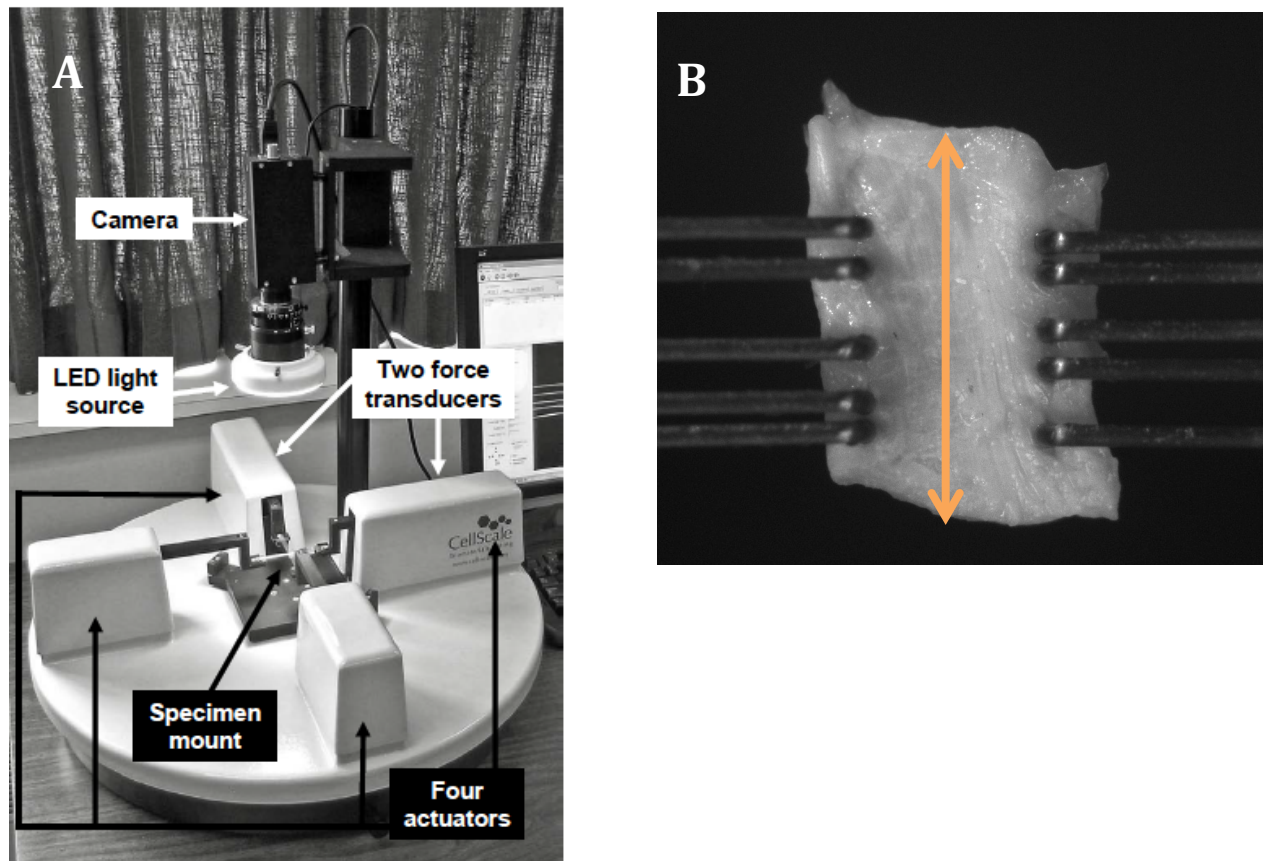
Figure 13. (A) Biotester 5000 (Cellscale, Waterloo, Ontario), (B) ovine single layer tissue loaded in the Biotester 5000, indicating orientation of fibres (orange arrow) within the sample.

period followed the testing protocol. LabJoy software was used to record force and displacement

for each test, where data were collected at 100Hz.

2.1.3 Data Analysis

Strain values (%) were calculated by dividing displacement values (mm) by the original

length of the tissue (mm) when loaded in the BioTester5000 apparatus (Figure 8):

$$1. \quad Strain = \frac{displacement}{original\ length} x\ 100\%$$

Stress values (MPa) were calculated by dividing force (MPa) by cross-sectional area of

the tissue (mm^2). Cross-sectional area was obtained by multiplying tissue width (mm;

determined from laser displacement sensor) with tissue height (mm). Height values were

obtained using ImageJ software. Values were then divided by 1000 to obtain MPa values. Stress

was calculated using the following equation, where force was measure in mN and tissue height

and width were measured in mm:

$$2. \quad Stress = \frac{force/(tissue\ height\ x\ tissue\ width)}{1000}$$

Values for toe-region stress/strain, elastic region slope (elastic modulus), initial failure

stress/strain, and ultimate failure stress/strain were determined based on landmarks of a typical

stress-strain curve (Figure 6). The toe-region area was from the beginning of curve (i.e. at 0

stress/strain) to the point on the curve where linear stress/strain begins. The toe-region is marked

by an initial curvature of the graph. Elastic modulus was determined by calculating the slope of

the area on the graph with the longest linear relationship (elastic region). Initial failure was

marked by either a sudden decrease in stress, or a change in slope from the elastic region. The

ultimate failure stress/strain values were determined by the highest value of stress that the tissue

reached during the testing protocol, and its corresponding strain value.

2.2 Geometric and Hydration Protocols

2.2.1 Geometric Measurements

2.2.1.1 Height Ratios

Intact (unsegmented) frozen spines were imaged using a Mercury Modular X-ray and

processed using Kodak imaging software. Images were taken in both the frontal and sagittal

plane for all spines (Figure 14). ImageJ software was used to obtain values for IVD and vertebral

heights for a total of 4 IVDs and 4 vertebrae for porcine and ovine specimens, and 3 IVDs and 3

vertebrae for bovine specimens (see table 8 for sample total). Three measurements each of

anterior and posterior, and six measurements of lateral IVD and vertebrae heights were obtained

and averaged for a total IVD and vertebral height in the anterior, posterior, and lateral planes.

Coefficient of variation (standard deviation normalized by the mean) was determined for each

variable measured and ranged from 1% to 9% variation across the three repeated measures. Total

IVD and vertebral heights were calculated by averaging all IVD and vertebral heights taken
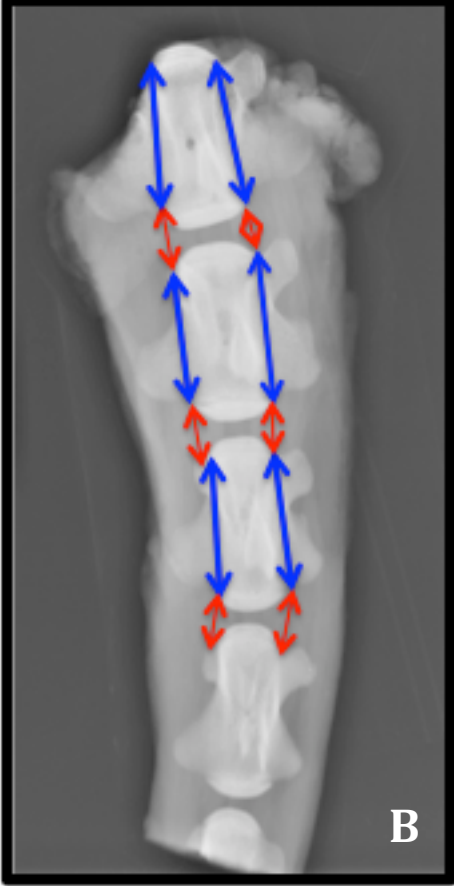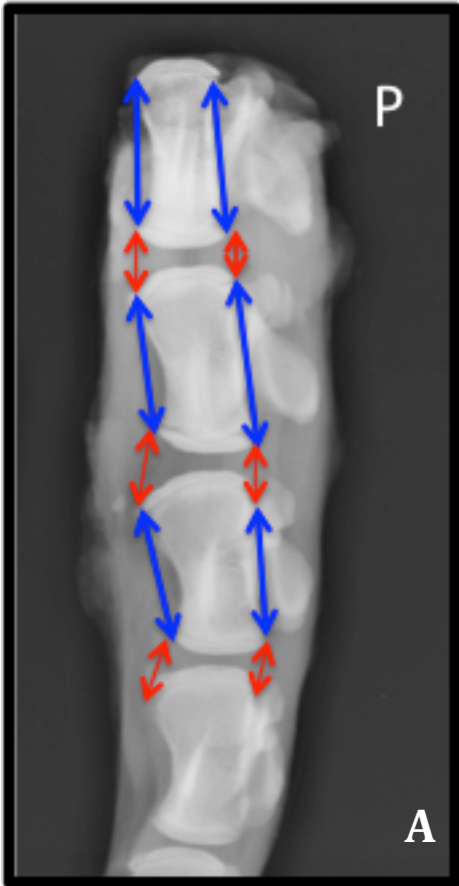
Figure 14. X-Ray images of a bovine tail in the sagittal (A) and frontal (B) planes, indicating where measurements were taken for intervertebral disc and vertebral height ratio calculations. Porcine (C) and ovine (D) images taken in sagittal plane. Blue arrows indicate the vertebral heights, red arrows indicate the IVD heights. *P* represents the posterior spine.

Table 8. Distribution of sample size used for height ratio measurements of bovine tail, porcine lumbar, and ovine lumbar intervertebral discs and vertebrae. Ratios represent a single intervertebral disc and the most cranial adjacent vertebrae.

Species	# Ratios taken per spine	# Spines	Total
Bovine	3	5	15
Porcine	4	5	20
Ovine	4	4	16
			N= 51

(anterior, posterior, and lateral measurements). IVD: vertebral height ratios were obtained by

comparing the average IVD height to the vertebral height cranial to the IVD (Figure 14).

2.2.1.2 Width Ratios

Width measurements were taken in the anterior-posterior and lateral planes (Figure 15)

using digital calipers. A-P: lateral width ratios were then calculated. Geometric measurements

were taken from a single disc per spine that was subsequently used for histological analysis;

IVDs were randomly assigned for width ratio protocol. Measurements were taken after excision

from the spine, but prior to histological preparation. See Table 9 for sample size distribution.

2.2.2 Water Content

A second IVD from each spine was excised by cutting the disc at the vertebral endplate;

IVDs were randomly assigned for water content protocol. A total of 15 IVDs were used to

calculate whole IVD water content: one IVD per spine, five spines per species. IVDs were

excised while frozen to ensure that all IVD content was removed during dissection. Once

removed, IVDs were immediately wrapped in plastic wrap and lightly sprayed with PBS until

fully thawed to reduce hydration loss in the IVD (Pflaster et al., 1997). The amount of PBS

sprayed on the IVD was negligible and did not contribute significantly to the weight of the IVD

before desiccation of the tissue.

Anterior
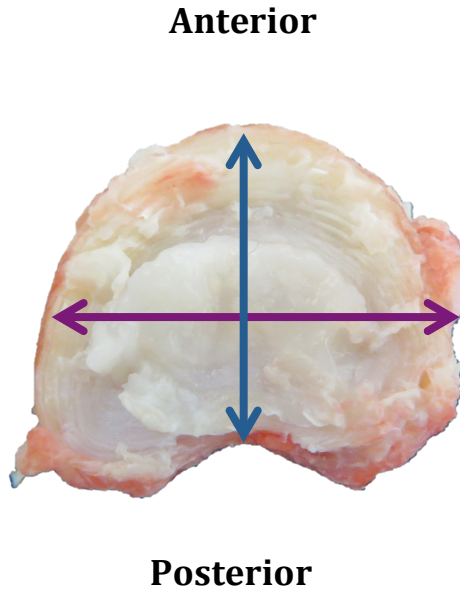
Posterior

Figure 15. Ovine lumbar intervertebral disc with arrows indicating anterior-posterior (blue arrow) and lateral (purple arrow) widths used to calculate width measurement ratio.

Table 9. Distribution of sample size for bovine tail, porcine lumbar, and ovine lumbar intervertebral discs used for anterior-posterior: lateral width ratio calculations.

Species	# Discs per spine	# Spines	Total
Bovine	1	5	5
Porcine	1	5	5
Ovine	1	5	5
			N= 15

IVDs were weighed before incubation to obtain wet weight values (g), and subsequently incubated at 65 °C for 24 hours using a Barnstead Thermolyne incubator (Sigma-Aldrich, St. Louis, MO). After the protocol, IVDs were weighed to obtain dry weight (g) after desiccation. Water weight (g) was determined by subtracting dry weight from wet weight. Water content was then calculated using the following equation to normalize all values and expressed in mL/g dry weight:

$$3. \ \boldsymbol{Water\ content} = \frac{water\ weight - dry\ weight}{wet\ weight - dry\ weight}$$

Percent water content was calculated using the following equation:

$$4. \ \% \boldsymbol{Water\ content} = \frac{wet\ weight - dry\ weight}{wet\ weight}$$

2.3 Histological Protocol

2.3.1 Tissue Preparation

A third IVD from each spine was randomly assigned for histological analysis and completely excised from adjacent vertebrae. IVDs were removed while frozen for ease of dissection. Once removed, anterior-posterior and lateral width measurements were recorded and the IVD was subsequently cut into two halves in the anterior-posterior plane. Each half IVD contained anterior, lateral, and posterior segments of the IVD, as well as outer AF, inner AF, and

NP. IVDs were placed in histological cassettes in the desired orientation and rinsed with 70%

alcohol and/or PBS to remove any excess IVD or connective tissue. IVDs were then fixed in

10% buffered formalin for a period of approximately 7-10 days. After this time, IVDs were

trimmed superiorly and inferiorly using a microtome blade to ensure smooth surface for slide

preparation. Staining and slide preparation was conducted at the Ontario Veterinary College

Animal Health Laboratory at the University of Guelph in Guelph, Ontario.

2.3.2 Histological Staining

Three stains were chosen based on their ability to detect desired cells and ECM

structures, as well as for their use in previous literature pertaining to IVD histology:

1. *Safranin-O/ fast green* (McCann et al., 2013; Sun et al., 2012; Leung et al., 2009)

This stain is used to detect sulfated glycosaminoglycans chains of proteoglycans,

including chondroitin sulfate and keratin sulfate. Safranin-O stained proteoglycans red,

using fast green as a contrast stain. Although fast green is typically used to detect

collagen, it was not used to identify collagen in the tissues. Rather, its purpose was as a

contrast stain to safranin-O.

2. *Hematoxylin and eosin (H & E)* (Tampier, 2006; Errington et al., 1998)

The use of the H & E stain was twofold. The first use was to detect collagen type

I and II, staining type I pink and type II purple. Secondly, H & E is commonly used to

stain the nuclei of cells black. Identification of the cells was based of morphological features of the cell types, such as size and shape of nuclei and cytoplasm.

3. *Triple dye method (Weigert's hematoxylin, picrosirius red, alcian blue)* (Gruber et al., 2002)

The combination triple dye stain was developed by Gruber et al. (2002) specifically for IVDs to enhance the histological resolution of the tissue. This combination stain allowed for a better visual contrast of the structures. Collagens were stained red, proteoglycans (both sulfated and non-sulfated) were stained blue, cell nuclei were stained blue-black, and other tissue elements were stained yellow.

2.3.3 Cell Counts and Identification

2.3.3.1 Equipment

Histological slides were viewed using the Axiolab microscope (Zeiss, Jena, Germany) and images used for analysis were taken with the Inifinity 1 camera (Lumenera, Ottawa, Ontario). Slides used for figures and cell counts were scanned at 20x using the NanoZoomer Digital Slide Scanner (Hamamatsu, Hamamatsu City, Japan) at The Toronto Centre for Phenogenomics in Toronto, Ontario, and viewed using Hamamatsu NanoZoomer Digitial Photography software (Hamamatsu, Hamamatsu City, Japan).

2.3.3.2 Cell Identification

Identification of cells types were based on previous described morphological features of

IVD cells (Trout et al., 1982; Maroudas et al., 1975; Errington et al., 1998; Chelberg et al. 1995;

Zhou et al., 2008; Bruehlmann et al., 2002; Postacchini et al., 1984) and verified with a

molecular biologist at UC San Diego (Rajeswarti Pichika, PhD). Fibroblast-like cells were

characterized by having long narrow nuclei with a relatively small cytoplasm, chondrocyte-like

cells were characterized by having oval nuclei and an overall oval shape, and notochordal cells

were characterized by having a large, rounded cytoplasm and round nuclei.

2.3.3.3 Cell Count

Using NanoZoomer Digital Photography software (Hamamatsu, Hamamatsu City, Japan)

squares of equal area were drawn on the scanned images of the histological slides and cell

counts were obtained by counting the amount of nuclei in this given area. Three different areas

were counted per region of the IVD (outer AF, inner AF, and NP).

2.4 Statistical and Data Analysis

2.4.1 Biomechanical Data

A two-way ANOVA was used to determine statistical significance. Two factors were

considered: species type (three levels: bovine, porcine, ovine) and location (two levels: anterior,

posterior). An alpha level was set at 0.05, and a Tukey HSD post hoc test was used if a statistically significant result was found.

2.4.2 Geometric and Anatomic Data

A one-way ANOVA was used to determine statistical significance for water content, geometric measurement ratios, and cell counts between species (3 levels: bovine, porcine, ovine). An alpha level was set at 0.05 and a Tukey HSD post hoc test was used if a statistically significant result was found.

2.4.3 Percent Deviation

The percent deviation of the models from human data presented in literature was calculated using the following equation:

$$5. \ \%\ deviation = \frac{model\ species - human}{human}$$

Chapter 3:

Results

3.1 Tensile Testing

The tensile properties of single lamellae were tested using the BioTester 5000 (Cellscale, Waterloo, On). The tissues were loaded onto rakes, which then pierced the tissue and subsequently pulled the layers perpendicular to its fibre orientation. Fifty-three single layers tissues were tested and all but eight tissues (85%) reached ultimate failure. Ovine single layers comprised three quarters of the tissues that did not reach ultimate failure (6 tissues: 4 anterior, 2 posterior), whereas the remaining 2 samples (1 anterior, 1 posterior) were from porcine spines. All bovine tissues reached ultimate failure.

3.1.1   Strain and Stress

Generally speaking, the overall trend for all biomechanical variables was that the bovine and the ovine tissues differed the most from one another, and the porcine model was intermediate between the other models. Ovine tissues tended to deform more (reach higher strains) at the end of the toe region, initial failure, and ultimate failure, whereas the bovine tail tissues did not deform as much as the other two models at the same points in the stress-strain curve. Conversely, bovine tissues exhibited higher stresses at the end of the toe region, initial failure, and ultimate failure, whereas the ovine exhibited the lowest stress values (Table 10).

Differences observed between the strain values reached at the end of the toe region, at initial failure and at ultimate failure were consistent across species (Figure 16). The intralamellar

Table 10. Strain, stress values at the end of the toe-region, initial failure, and ultimate failure, and elastic modulus for bovine tail, porcine lumbar, and ovine lumbar after tensile testing of intralamellar region of single layers of annulus fibrosus.

Species	End of Toe Region Strain (%) (SD)	End of Toe Region Stress (MPa) (SD)	Elastic Modulus (MPa) (SD)	Initial Failure Stain (%) (SD)	Initial Failure Stress (MPa) (SD)	Ultimate Failure Strain (%) (SD)	Ultimate Failure Stress (MPa) (SD)
Bovine	21.2 (21.9)	0.09 (0.08)	1.88 (1.26)	50.0 (33.8)	0.50 (0.35)	93.9 (51.8)	0.77 (0.48)
Porcine	27.7 (25.3)	0.09 (0.09)	0.87 (0.61)	71.6 (45.3)	0.48 (0.39)	111.9 (60.2)	0.70 (0.52)
Ovine	36.3 (31.6)	0.05 (0.04)	0.47 (0.38)	103.6 (53.3)	0.28 (0.19)	153.6 (52.7)	0.39 (0.19)
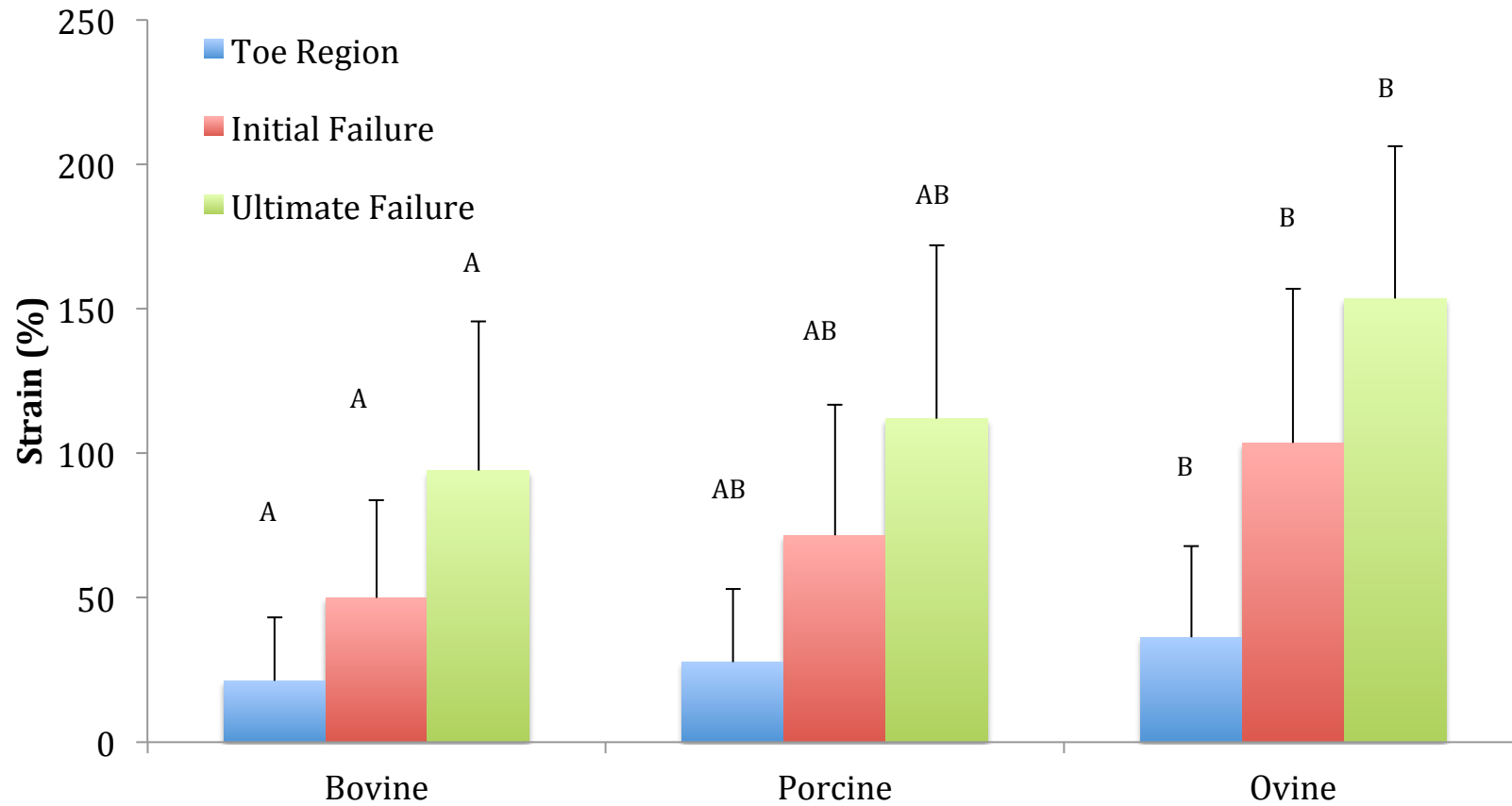
Figure 16. Strain values (observed deformation relative to size of initial tissue) for bovine tail, porcine lumbar, and ovine lumbar models at the end of toe-region, initial failure, and ultimate failure of intralamellar region of single layers of annulus fibrosus. Different letters indicate significance between species. N= 53, one-way ANOVA.

strain values significantly differed between species (p= 0.0165), where the bovine and the ovine single layers differed the most from one another (p= 0.0127), but neither were significantly different from the porcine model. This was consistent for all tensile strain values (toe-region, initial failure, and ultimate failure). No significant differences were found for the strain values between the anterior or posterior tissues (p>0.05 for each strain variable). However, when both species type and location of the tissue was considered, a significant interaction (p= 0.0287) was found for the toe-region strain (Figure 17). The anterior tissues from the bovine exhibited higher strain values than tissues extracted from the posterior, where as in the porcine and ovine, posterior tissues exhibited higher strains that anterior tissues (Figure 17).   No significant interaction was found between species type and location for initial (p= 0.585) or ultimate failure (p= 0.626). In general, the ovine tissues displayed the highest strain, and the bovine tissues displayed the lowest strain; the porcine tissue values were intermediate.

Stress values revealed differences between species (Figure 18) as well as sample location. No significant difference was found between species for the stress values seen at the end of the toe-region, however, the location of the tissue did produce a significant result (p= 0.01) with higher stress values for the posterior tissues (0.10 ± 0.09 MPa) than the anterior tissues (0.05 ± 0.04 MPa). Significant differences were seen between species at both initial failure (p= 0.044) and ultimate failure (p= 0.025). It was found that the ovine and bovine differed the most from
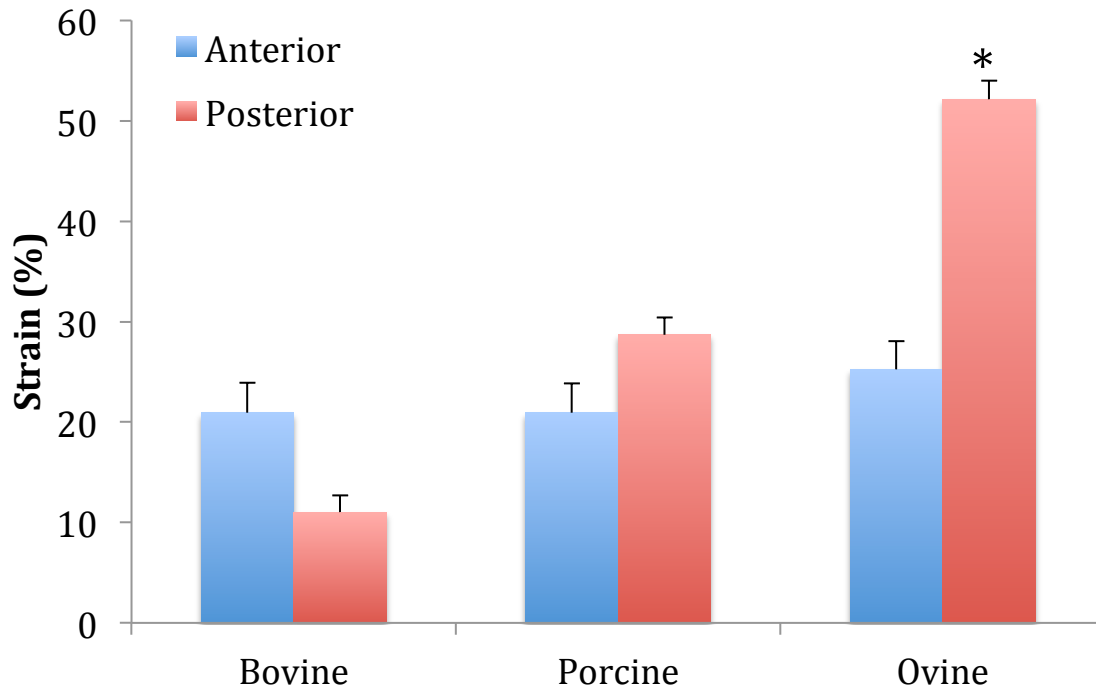
Figure 17. Interaction between species type and location (anterior versus posterior) of tissue for toe-region strain (observed deformation of tissue relative to initial size, during region when fibres are "uncrimping") of intralamellar region of single layers of annulus fibrosus. Standard error reported. (*) represents significantly different values, N= 53, two-way ANOVA
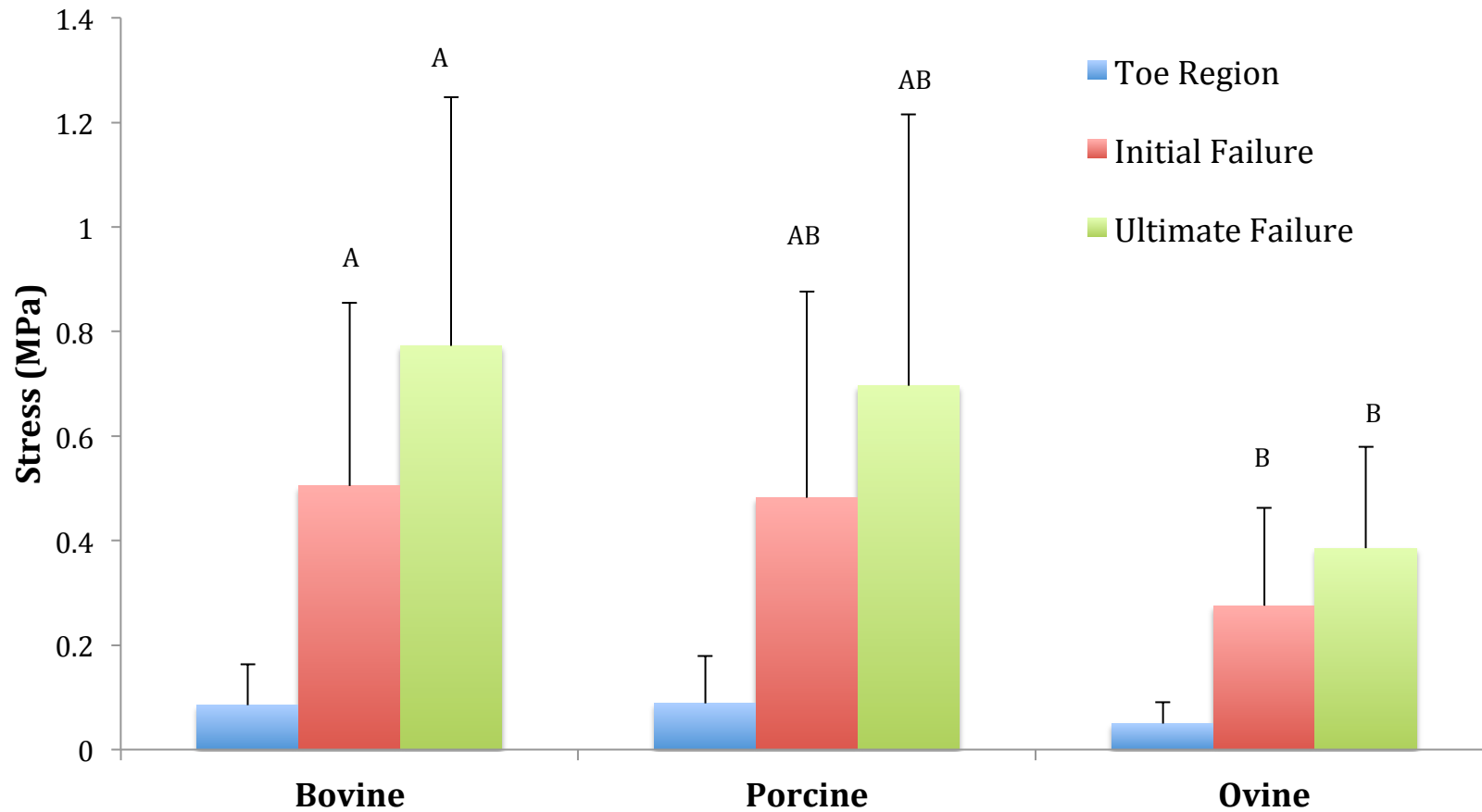
Figure 18. Stress (force/area; mN/mm^2 or MPa) values for bovine tail, porcine lumbar, and ovine lumbar intervertebral discs at the end of toe-region, initial failure, and ultimate failure of single layer annulus fibrosus. Different letters indicate significance differences between species. N= 53, one-way ANOVA.

one another at both initial failure (p= 0.040) and ultimate failure (p= 0.019) stress values, but were not different from the porcine model. In contrast to strain values, the bovine displayed the highest stress values, and the ovine displayed the lowest; porcine was again the intermediate model between the species. Similarly to the toe-region, the location of the tissue was found to be significantly different between the anterior and posterior samples at initial failure (p= 0.008) and ultimate failure (p< 0.001). Posterior tissues were found to fail at higher stresses (0.55 ± 0.35 MPa) than anterior tissues (0.32 ± 0.26 MPa), There was no significant interaction between species and location of the tissue for toe-region stress, initial failure stress, and ultimate failure stress.

3.1.2 Elastic Modulus

Elastic Modulus, or the stiffness of the tissue, was found to be significantly different between species (p< 0.001) (Figure 19) and between the location of the tissue (p= 0.03). Particularly, the bovine single layer tissues were stiffer than both the ovine and porcine samples (p< 0.001 for both porcine and ovine); no stiffness differences were found between the porcine and the ovine samples. The average stiffness of the bovine tail was found to be 1.88 ± 1.26 MPa, which was 2-3 times stiffer than either the porcine or the ovine models, which displayed a stiffness of 0.86 ± 0.61 MPa and 0.47 ± 0.38 MPa, respectively. Posterior samples had a greater
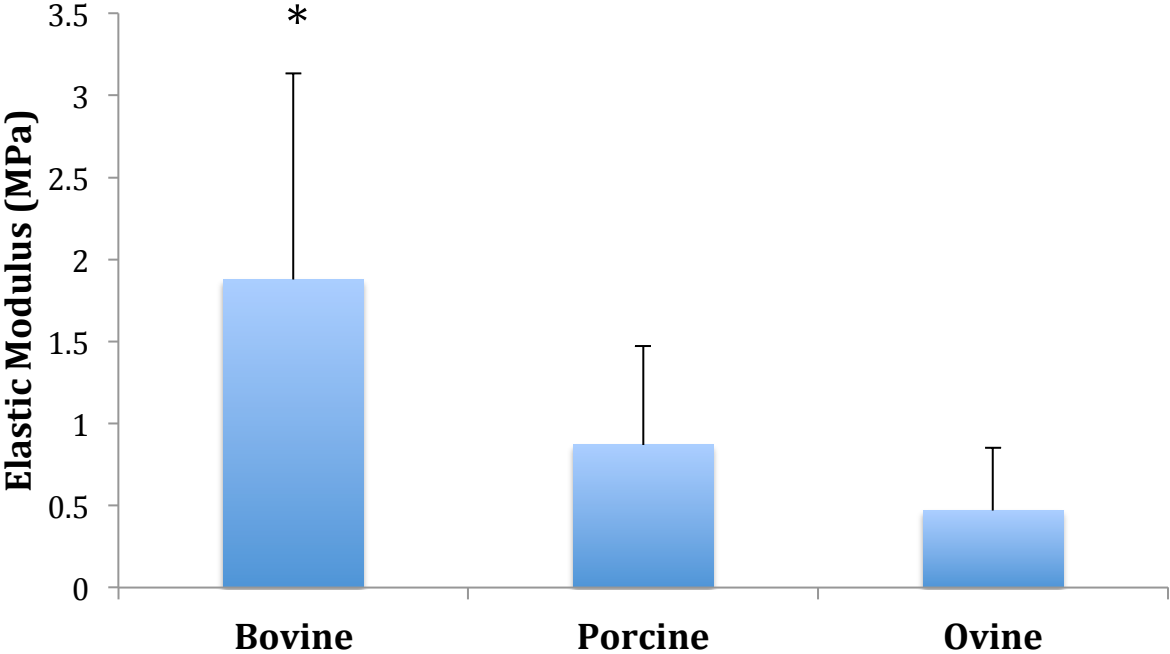
Figure 19. Elastic modulus (stiffness of tissue; ratio of stress to strain) for bovine tail, porcine lumbar, and ovine lumbar of intralamellar regions of single layers of annulus fibrosus. (*) represents significantly different values. N= 53, one-way ANOVA.

elastic modulus (1.53 ± 1.13 MPa) than tissues extracted from the anterior IVD (0.72 ± 0.69

MPa). No significant interaction between species and location of the tissue was observed.

3.2 Geometric and Hydration Measurements

3.2.1 Geometric Ratios

When comparing IVD: vertebral height ratio, a significant difference was found between

all species (p< 0.001), where each species displayed its own unique height ratio (Figure 20). The

bovine tail differed from both the porcine and ovine (p< 0.001) models, and similarly, the

porcine and the ovine spines differed from one another (p= 0.003). The ovine spine was found to

have the smallest height ratio (0.14 ± 0.02), whereas the bovine had the largest height ratio (0.34

± 0.03). The porcine spine displayed an intermediate ratio of 0.21 ± 0.02). Further analysis of the

data found that the IVD heights were significantly different between the models (p< 0.01), but

not the vertebral heights (p> 0.05).

Width ratios revealed a significant difference between species (p< 0.001), however, only

the bovine tail differed the most from the other two models (Figure 21); p< 0.001 for both

porcine and ovine. The average A-P: lateral width ratios were the greatest for the bovine tail

(1.02 ± 0.09) and lowest for the porcine lumbar (0.66 ± 0.04); the ovine lumbar had an
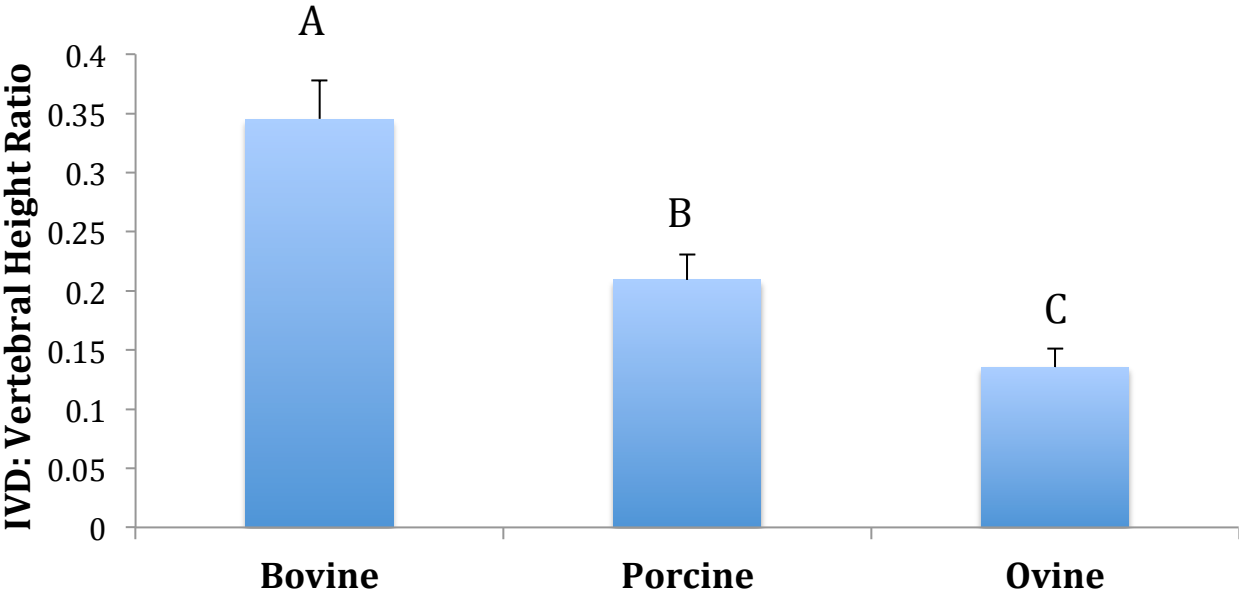
Figure 20. Intervertebral discs: vertebral height ratios of bovine tail, porcine lumbar, and ovine lumbar intervertebral discs. Letters represent significant differences. N= 51, one-way ANOVA.
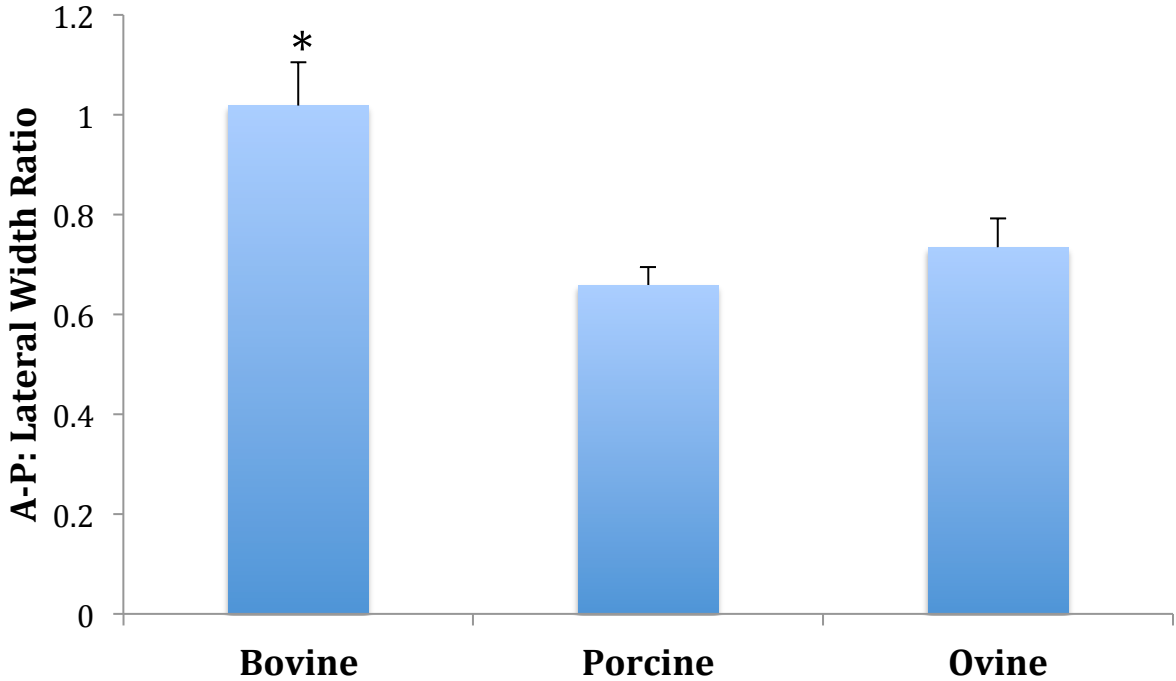
Figure 21. Anterior-posterior: lateral width ratios of bovine tail, porcine lumbar, and ovine lumbar intervertebral discs. (*) represents significant differences. N= 15, one-way ANOVA.

intermediate ratio (0.74 ± 0.06) between the two other species. See table 11 for absolute IVD and vertebral height, and width measurements.

3.2.2 Water Content

No significant differences were found in whole IVD water content between the species (p= 0.149). The average water content for the bovine, porcine, and ovine IVDs was 2.8 ± 0.3 mL/g dry weight, 2.34 ± 0.2 mL/g dry weight, and 2.57 ± 0.35 mL/g dry weight, and the average water mass was 2.75 ± 0.3, 2.34 ± 0.2, and 2.57 ± 0.4, respectively. The percent of water content in each IVD for bovine, porcine, and ovine was found to be 73.14 ± 2.4 %, 69.91 ± 2.1 %, and 71.79 ± 2.8 %, respectively.

3.3 Histological Analysis

3.3.1 Cell Counts and Types

All cells types (FBL, CCL, NC) were detected in the models, however, the distribution and cell count differed between models. In particular, the NP of the bovine tail had a significantly lower cell count (p< 0.001; 129 cells/ mm^2) than NP of the porcine (438 cells/ mm^2) and ovine (458 cells/ mm^2) IVDs (Figures 22 and 23). No significant difference was found in cell count for the outer AF and inner AF between species (outer AF: p= 0.22, inner AF: p= 0.91). Cell counts in the outer AF for the bovine, porcine, and ovine was 534 cells/ mm^2,

Table 11. Absolute height and width measurements, ratios, and water content for human lumbar, bovine tail, porcine lumbar, and ovine lumbar intervertebral discs. Standard deviation reported. Human gold standard values taken from [1]Buccher et al. (2010) and [2]Beckstein et al. (2008).

Species	IVD Height (mm)	Vertebral Height (mm)	IVD: Vertebral Height Ratio	A-P Width (mm)	Lateral Width (mm)	AP: Lateral Width Ratio	Water (%)
Human	11.02[1]	27.98[1]	0.39[1]	37.67[2]	55.38[2]	0.68[2]	77.67
Bovine	12.92 (0.37)	38.37 (3.00)	0.34	24.06 (1.23)	23.71 (23.71)	1.01	73.14
Porcine	7.81 (1.4)	37.14 (3.53)	0.21	25.01 (2.24)	38.02 (38.02)	0.66	69.91
Ovine	4.93 (0.44)	36.47 (1.63)	0.14	18.33 (1.75)	24.94 (1.69)	0.74	71.79
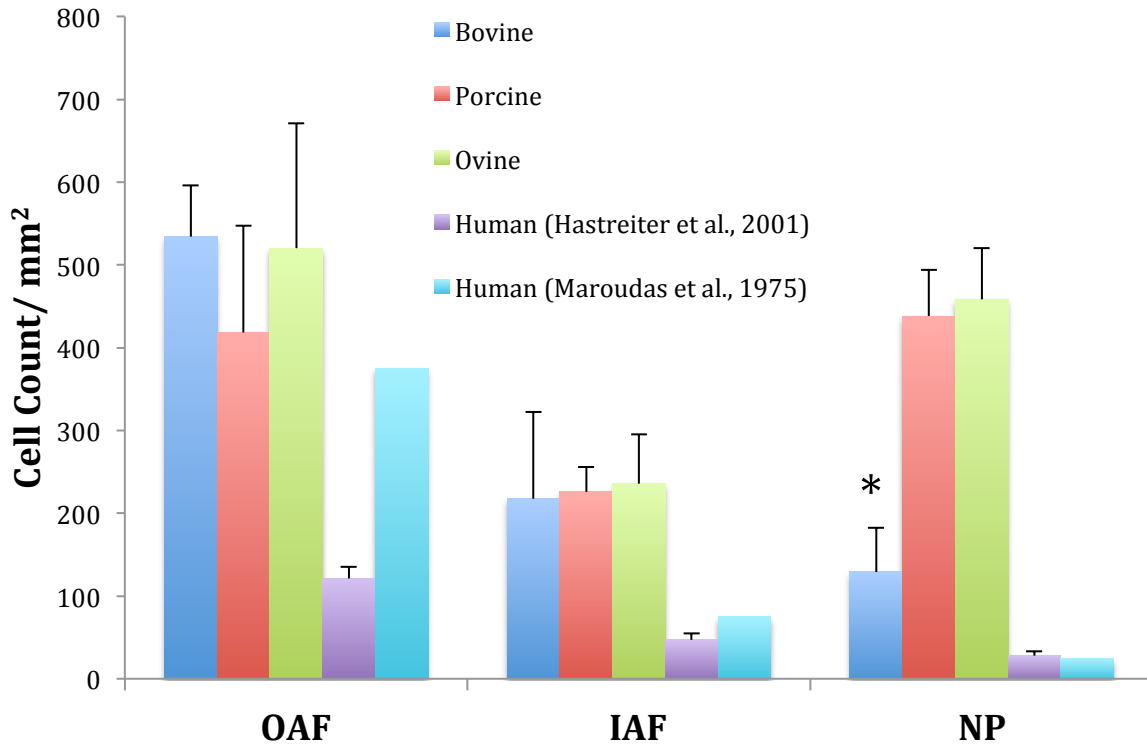
Figure 22. Cell count (cells/mm^2) in the outer annulus fibrosus (OAF), inner annulus fibrosus (IAF), and nucleus pulposus (NP) of bovine tail, porcine lumbar, ovine lumbar, and human lumbar intervertebral discs. Human data obtained from Hastreiter et al. (2001) and Maroudas et al. (1975). Error bars represent standard deviations; standard deviations not reported for Maroudas et al. (1975). (*) represent significantly different values; human data not included in statistical analysis.
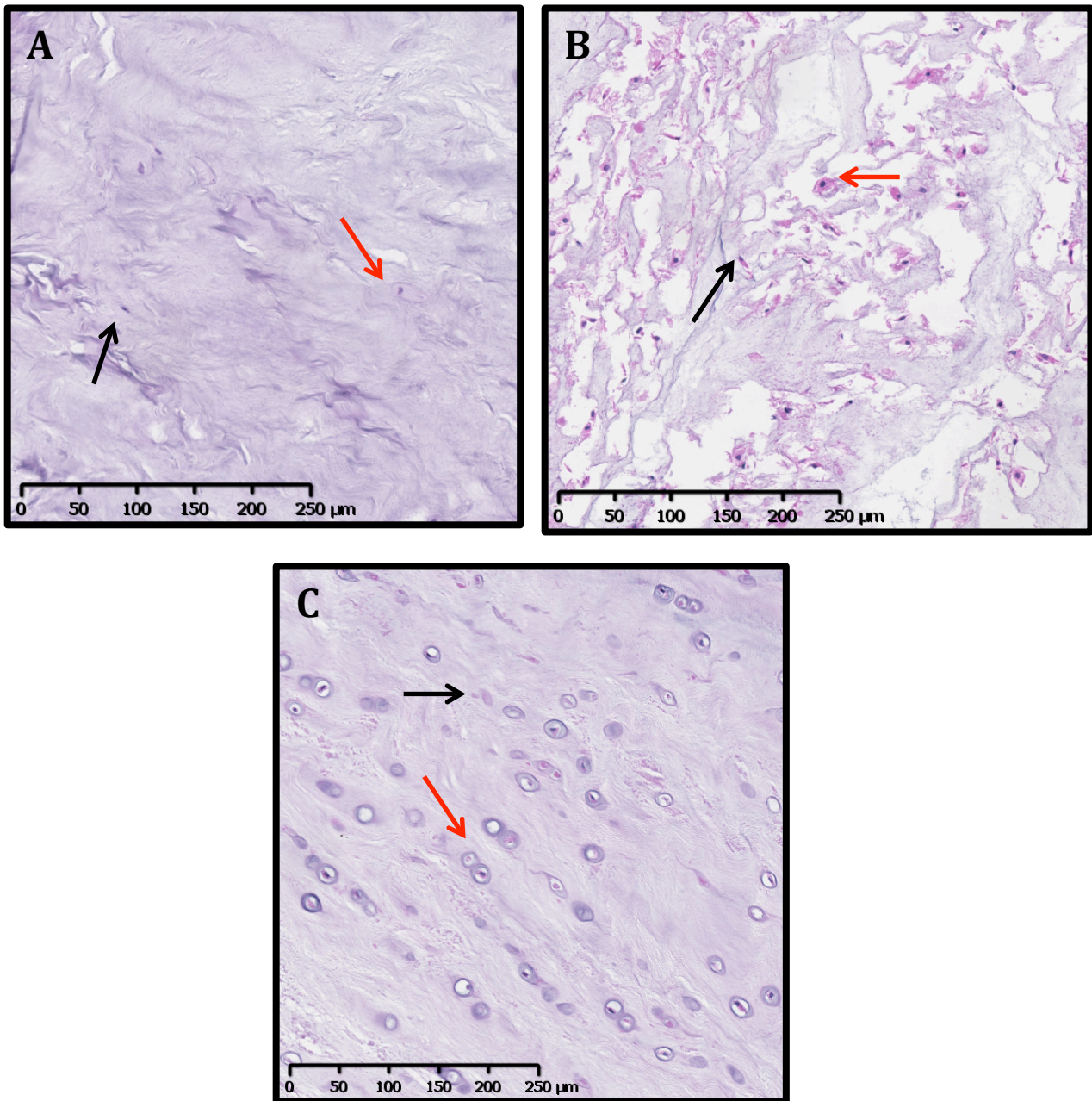
Figure 23. Sample densities of cells from the nucleus pulposus of bovine tail (A), porcine lumbar (B), and ovine lumbar (C) intervertebral discs indicating cell types. Chondrocyte-like cells indicated by black arrows, notochordal cells indicated by red arrows; collagen type I stained pink, collagen type II stained purple. H & E stain, 10.7x, scale bar: 250 μm.

418 cells/ mm^2, and 520 cells/ mm^2 (respectively), and 218 cells/ mm^2, 226 cells/ mm^2, 235 cells/ mm^2 (respectively) for the inner OAF.

As a general trend between species, the outer AF only contained FBL (which could be found singularly distributed or in rows, Figure 24) and the NP contained a mixture of CCL and NC. The inner AF showed the most variation in cell type present, especially in the transition zones between the outer AF and inner AF, and inner AF, and NP. There were, however, marked differences between the three species.

3.3.1.1 Bovine Tail

The bovine tail was predominantly dominated by FBL and CCL, with few NC. The density of FBL decreased drastically towards the NP after the first few layers of outer AF, and were only found in the outer AF. All cell types could be found residing between lamellae and running parallel to the orientation of the collagen fibres in rows (Figure 24). CCL were detected after the first few layers of the outer AF, and were present in the inner AF and NP. Very few NC were detected in the bovine tail, and, if present, were only found in the NP. The cell density decreased from the outer AF inwards towards the NP, which followed a similar trend to the decreasing cell count in the human IVD (Figure 22). The outer AF had the highest cell count in the bovine tail (534 cells/ mm2) compared to the other species (porcine: 418 cells/ mm^2; ovine: 520 cells/ mm^2).

3.3.1.2 Porcine Lumbar

Unlike in the bovine tail, cell types in the porcine IVD were not isolated to particular areas in of the IVD, making differentiation of the outer AF, inner AF, and NP less distinct. FBL were primarily found in the outer AF like the other models, however, few were also detected in
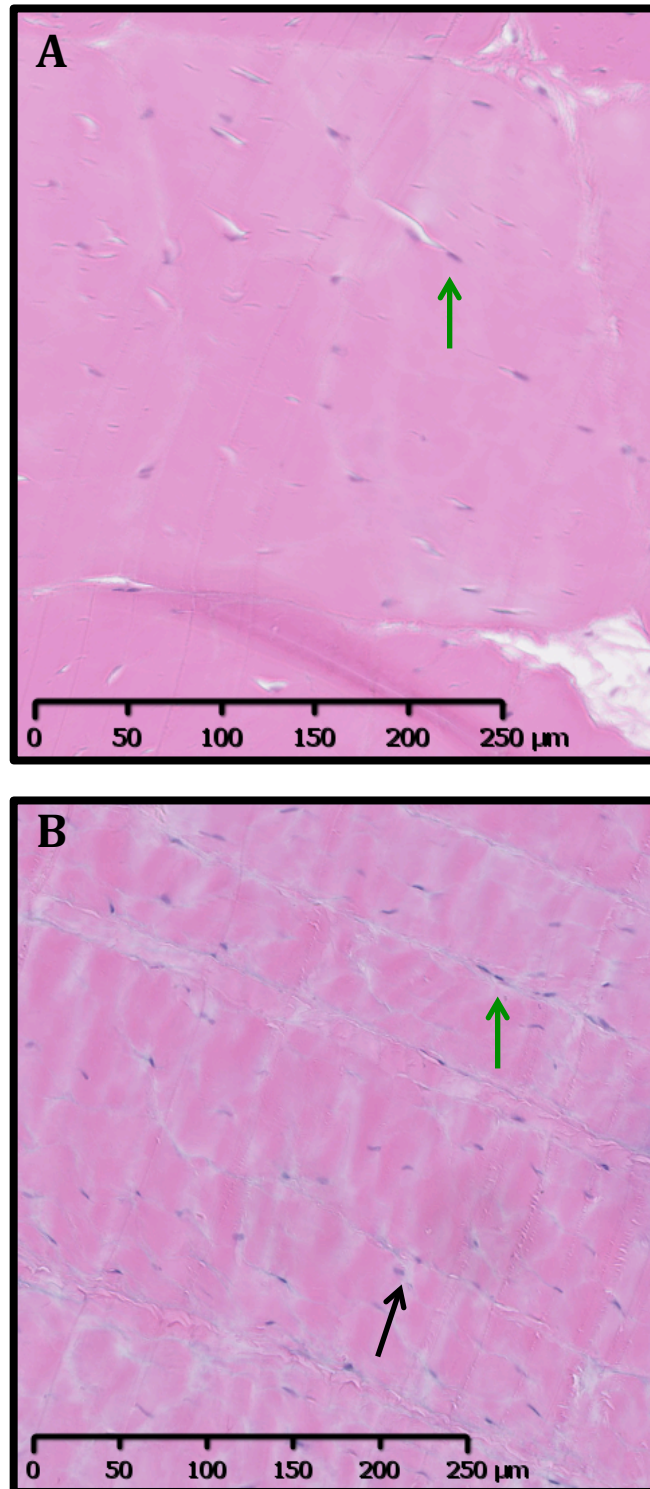
Figure 24. Arrangement of fibroblast-like cells (green arrow) in the outer annulus fibrosus, and fibroblast-like and chondrocyte-like (black arrow) in the inner annulus fibrosus (B) of the bovine tail. Note that the arrangement of fibroblast-like cells can be both singularly dispersed (A) and in rows (B). H & E, 11.7x, scale bar: 250 μm.

the inner AF. CCL began to emerge after the first few layers of the outer AF (middle AF). The inner AF was almost exclusively comprised of CCL, except for the lateral and medial peripheries of the inner AF, which contained trace amounts of FBL and NC, respectively. NC cells were found in the areas of the inner AF more medial to the NP, and throughout the NP (Figure 25). Additionally, CCL were found on the lateral periphery of the NP (Figure 25). Cell density in the NP was significantly higher in the porcine compared to the bovine ($p< 0.001$), but not significantly different than the ovine ($p= 0.811$). The cell density in the porcine was highest in the NP (438 cells/ mm^2), lowest in the inner AF (226 cells/ mm^2), and intermediate in the outer AF (418 cells/ mm^2).

3.3.1.3 Ovine Lumbar

Cells in the ovine IVD, regardless of type, appeared to be larger in size than the cells of the other models (refer to Figure 23 for size comparison). Much like the bovine tail, FBL were isolated to the outer AF (Figure 26). CCL and NC were present in the highest amounts and found at almost equal proportions within certain areas of the IVD. In the inner AF, CCL were more abundant than NC, however, NC were present in higher numbers than in the other models. The cell count in the NP was the highest in the ovine IVD (458 cells/ mm^2) than in the other two models (bovine: 129 cells/ mm2; porcine: 438 cells/ mm^2) and was significantly different than the bovine tail ($p< 0.001$), but not the porcine lumbar ($p= 0.881$). Within the ovine IVD, the lowest cell count was found in the inner AF, the highest cell count was found in the outer AF, and the NP cell count was intermediate between the two regions.

3.3.2 Extracellular Matrix Structures

Within the three regions of the IVD (outer AF, inner AF, NP) the presence and distribution of ECM structures was fairly consistent between species (Figures 27 and 28).
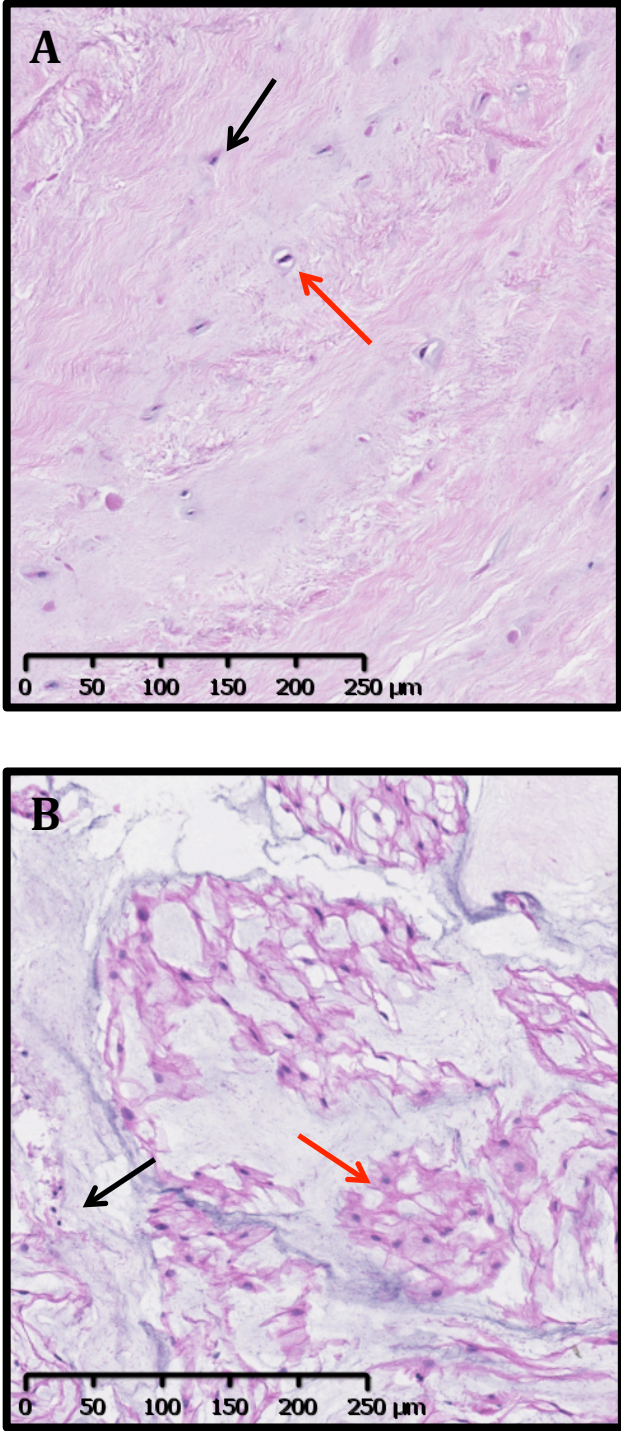
Figure 25. Outer periphery (A) and centre (B) of porcine nucleus pulposus indicating notochordal cells (red arrow) and chondrocyte-like cells (black arrow). Very few chondrocyte-like cells were found in the centre of the nucleus pulposus. H & E, 9.7x, scale bar: 250 μm.
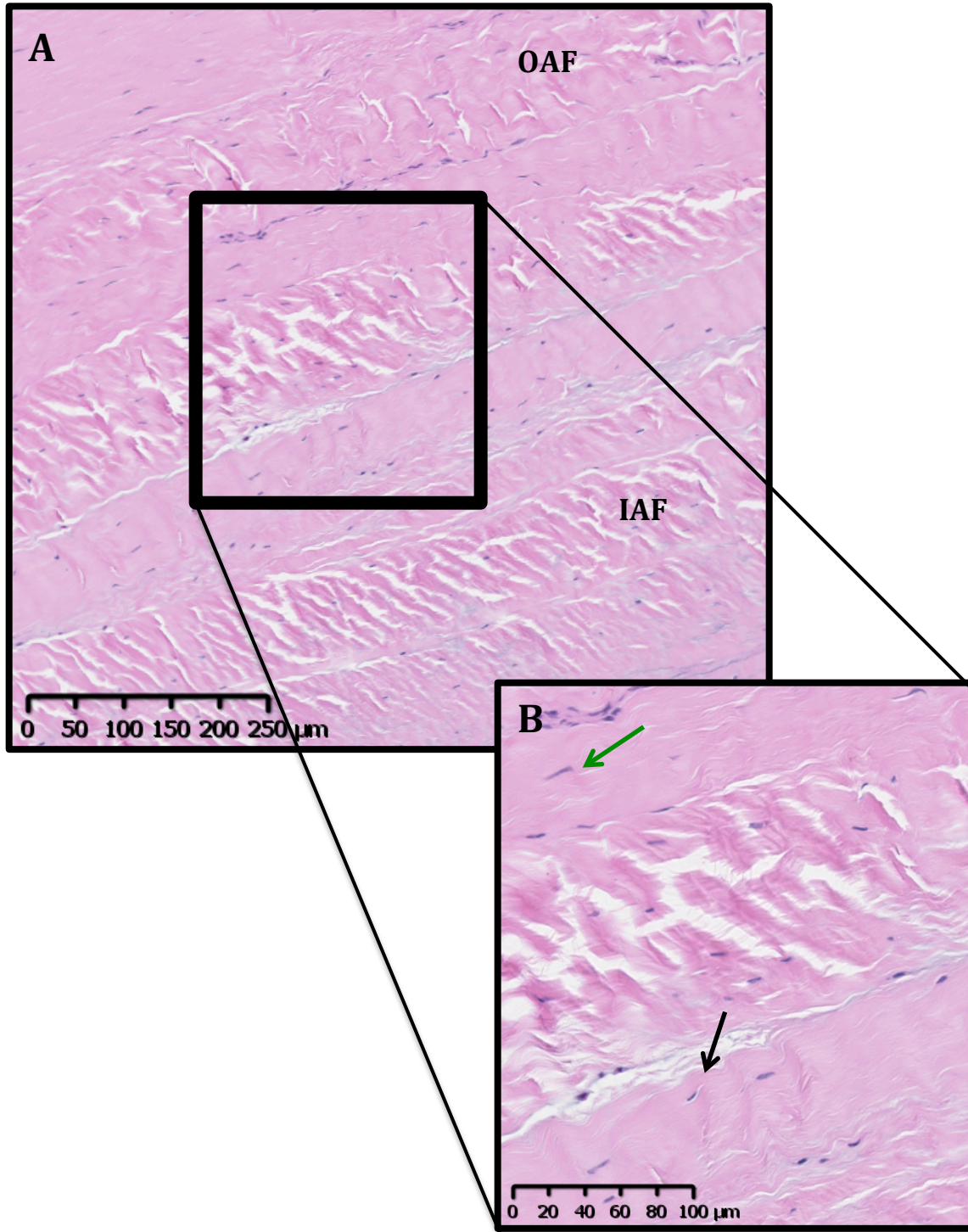
Figure 26. Outer annulus fibrosus (OAF) and inner annulus fibrosus (IAF) of ovine lumbar intervertebral disc indicating fibroblast-like cells (green arrow), which are isolated to outer annulus fibrosus, and chondrocyte-like cells (black arrow), which begin in inner annulus fibrosus; collagen type I stained pink, collagen type II stained purple. (B) Close up of separation of outer annulus fibrosus and inner annulus fibrosus based on cell types. H & E, (A) 6.63x, (B) 13.4x, scale bar: 250 μm (A), 100 μm (B).
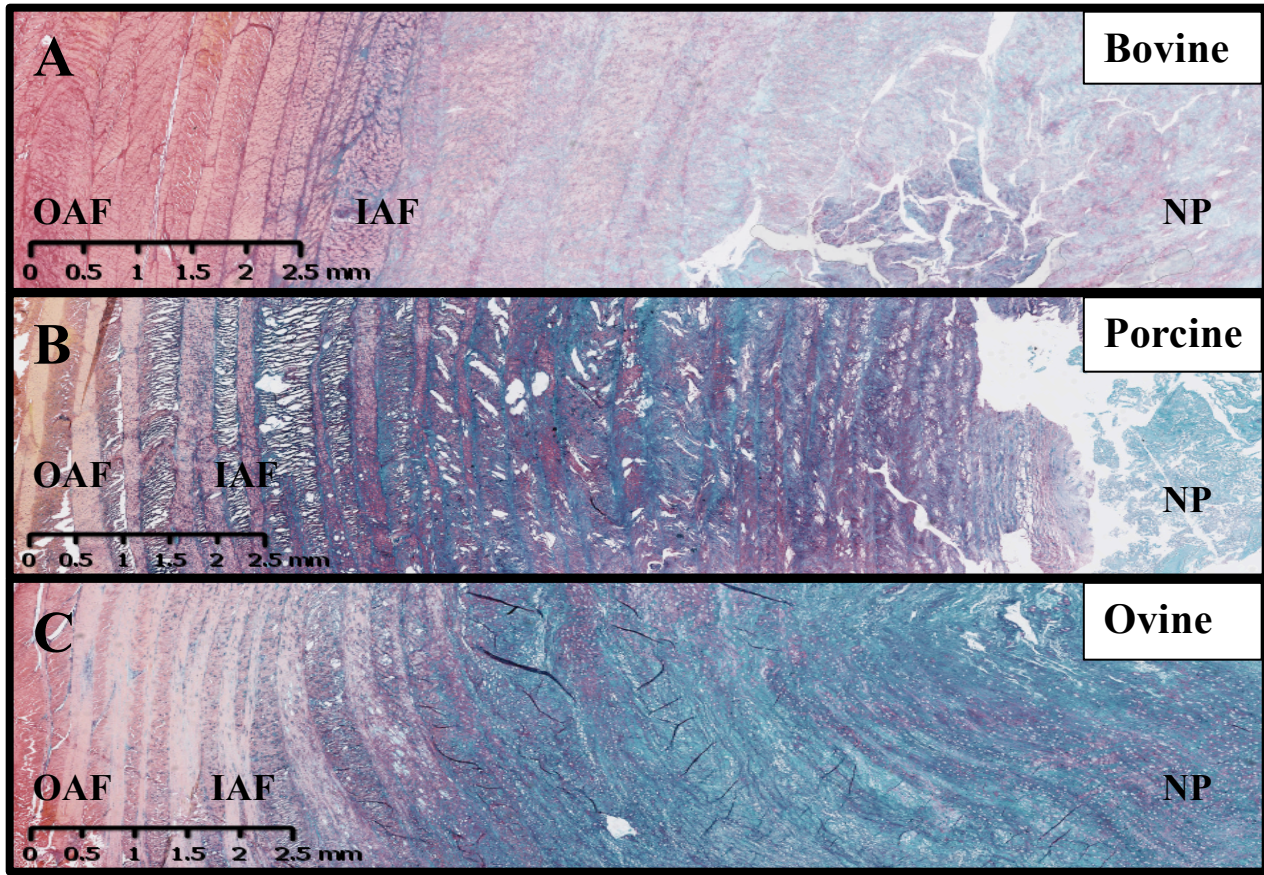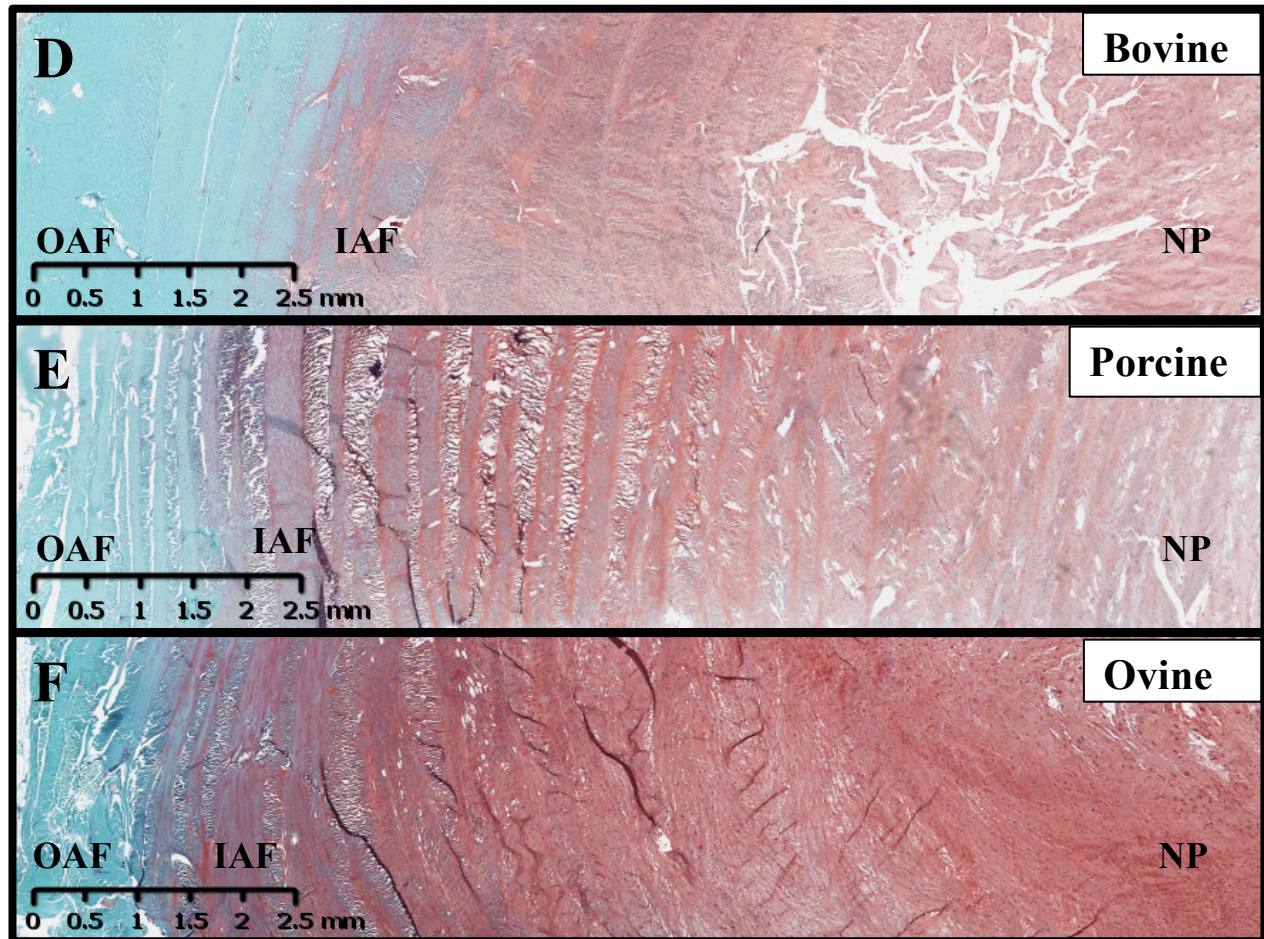
Figure 27. Stained intervertebral discs of bovine tail (A, D), porcine lumbar (B, E), and ovine lumbar (C, F) stained using a combination stain (Gruber, et al., 2004) (A-C) and safranin-O/fast green (D-F) showing the transition from outer annulus fibrosus (left) to nucleus fibrosus (right). The combination stain (A-C) stains collagen red and proteoglycans blue; safranin-O/ fast green (D-F) stains proteoglycans red. 0.67x, scale bar: 2.5 mm.

Bovine
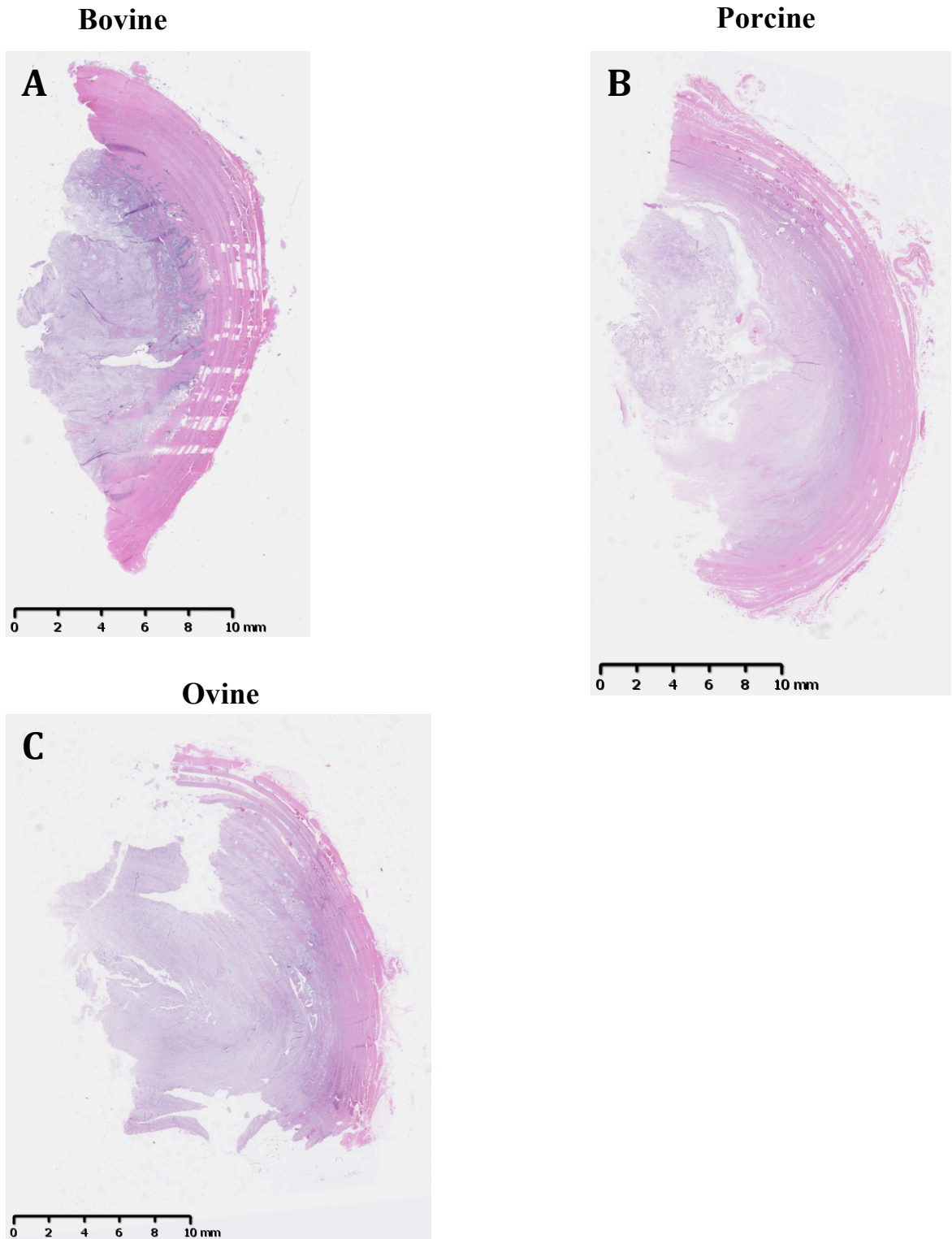
Porcine

Ovine

Figure 28. Intervertebral discs of bovine tail (A), porcine lumbar (B), and ovine lumbar (C) showing whole intervertebral disc distribution of collagen type I (pink) and type II (purple); H & E, (A) 0.27x, (B) 0.2x, (C) 0.23x, scale bar: 10 mm**.**

Differences in ECM structure abundance were found in the inner AF and NP, however, all species expressed the same ECM structures in each region.

The ECM composition of the NP was more similar between the porcine and ovine models than the bovine models, although each model had unique characteristics. The bovine tail had an almost equal distribution of collagen and proteoglycans in the NP, as indicated by the purple colour of the tissue (Figure 29A) In contrast, porcine NP was primarily saturated with proteoglycans with little to no collagen in the NP (Figure 29B). The concentration of collagen and proteoglycans in the ovine model was intermediate between the bovine and porcine (Figure 29C).

In all models, proteoglycans began to emerge in the first few layers of the inner AF and persisted into the NP. There did not appear to be a gradual transition from a collagenous to a more proteoglycan-rich matrix within the transition zone from the outer AF to the inner AF (Figure 27A,D). Rather, proteoglycans appear in the inner AF and persist into the NP at relatively similar proportions as collagen. This is not the case for the porcine or ovine models, where proteoglycan-rich areas can clearly been seen within the outer AF and NP, and within the transition zone a gradual transition from a more proteoglycan-rich matrix can be seen (Figure 27B,C,E,F).

Additionally, a "yellow" ring immediately following the first few layers of the outer AF was seen in all three models when stained with the Gruber method (Figure 27A-C); yellow indicates the presence of tissue elements other than collagen and proteoglycans. This area of "other tissue elements" was more distinct and larger in the porcine lumbar than in the other models.
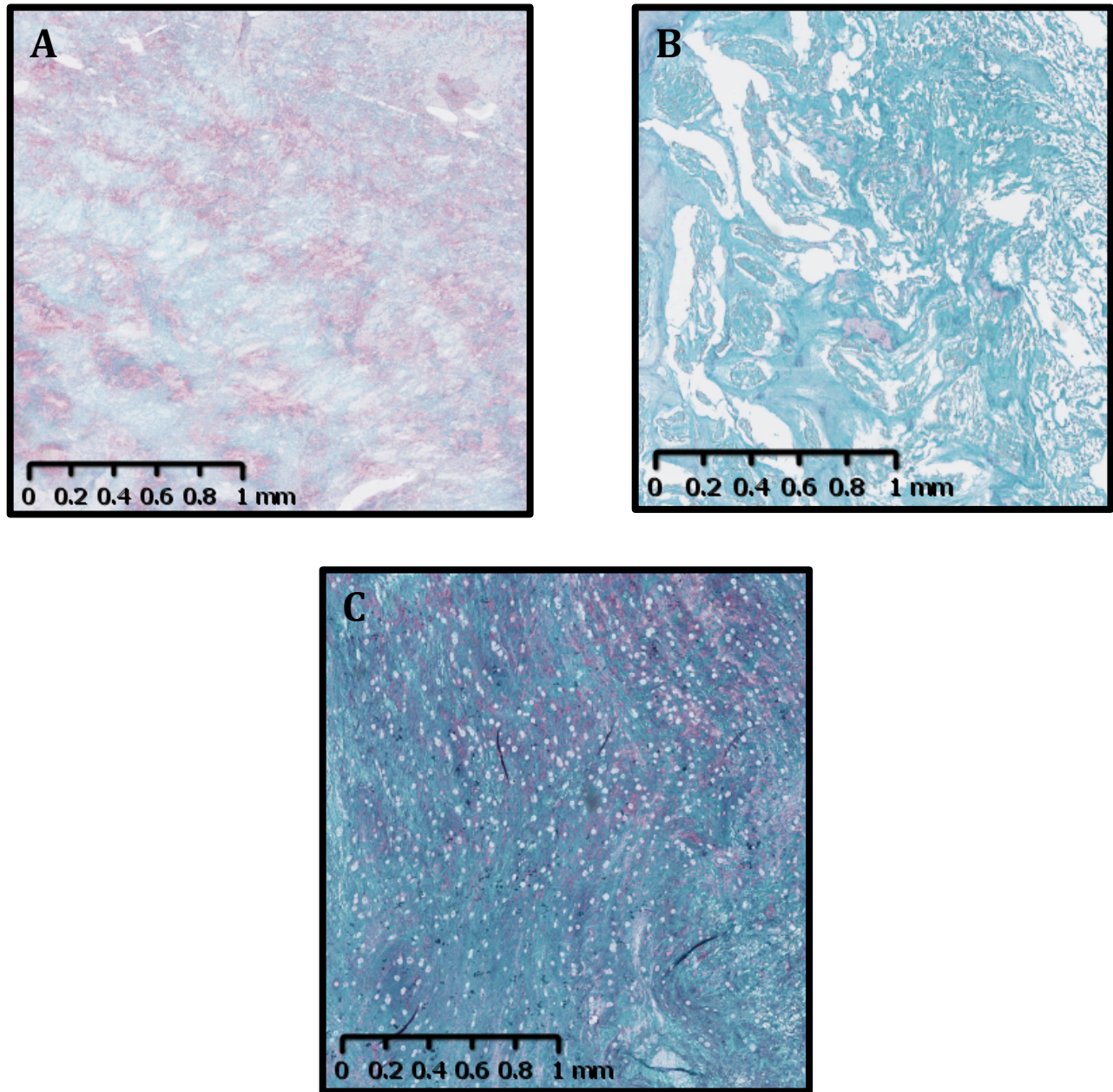
Figure 29. Nucleus pulposus of bovine tail (A), porcine lumbar (B), and ovine lumbar (C) intervertebral discs showing distribution of extracellular matrix proteins (collagen and proteoglycans) within the centre of the nucleus pulposus. Note the higher proportion of pink stain in the bovine tail indicating greater proportion of collagen content within the centre of the nucleus pulposus. Gruber combination stain, (B) 1.55x, (C) 1.46x, scale bar: 1 mm.

Very few differences were seen in the distribution of collagen types within the outer AF, inner AF, and NP. As a general trend, collagen type I was found only in the outer AF and collagen type II was found primarily in the inner AF and NP. Little to no collagen type II was found in the outer AF. In terms of collagen distribution, the porcine and ovine models appear to be the most similar. In the bovine tail, the transitional zone between the outer AF and inner AF was much larger than in the other models (Figure 28). Consequently, collagen type I persisted more medially towards the NP than in the other models. Additionally, the transition from collagen type I in the outer AF to collagen type II in the inner AF was more discrete in the bovine IVDs than in the other models, where in the porcine and ovine IVD there were larger areas of integration between the two types of collagen (Figure 28).

3.4 Human Data Comparison

Values for the elastic modulus of the intralamellar region of human single layer AF was 0.22 ± 0.2 (MPa) obtained from Holzapfel et al. (2005). The ratio of human IVD: vertebral height was calculated to be 0.39 from height values obtained from Busscher et al., 2010. Water content of human IVD was averaged between outer AF, inner AF, and NP from values obtained from Beckstein et al. (2008) and was found to be 77.67%. A-P: lateral width was calculated to be 0.68 from width values obtained from Beckstein et al., 2008.

Percent deviation of bovine, porcine, and ovine models from human values (Figure 30) for the elastic modulus were 755%, 296%, 114% (respectively), for IVD: vertebral height were -13%, -46%, -64% (respectively), for A-P: lateral width were 3%, 8%, 49% (respectively), and for water content were 5.85%, 9.99%, and 7.57% (respectively).
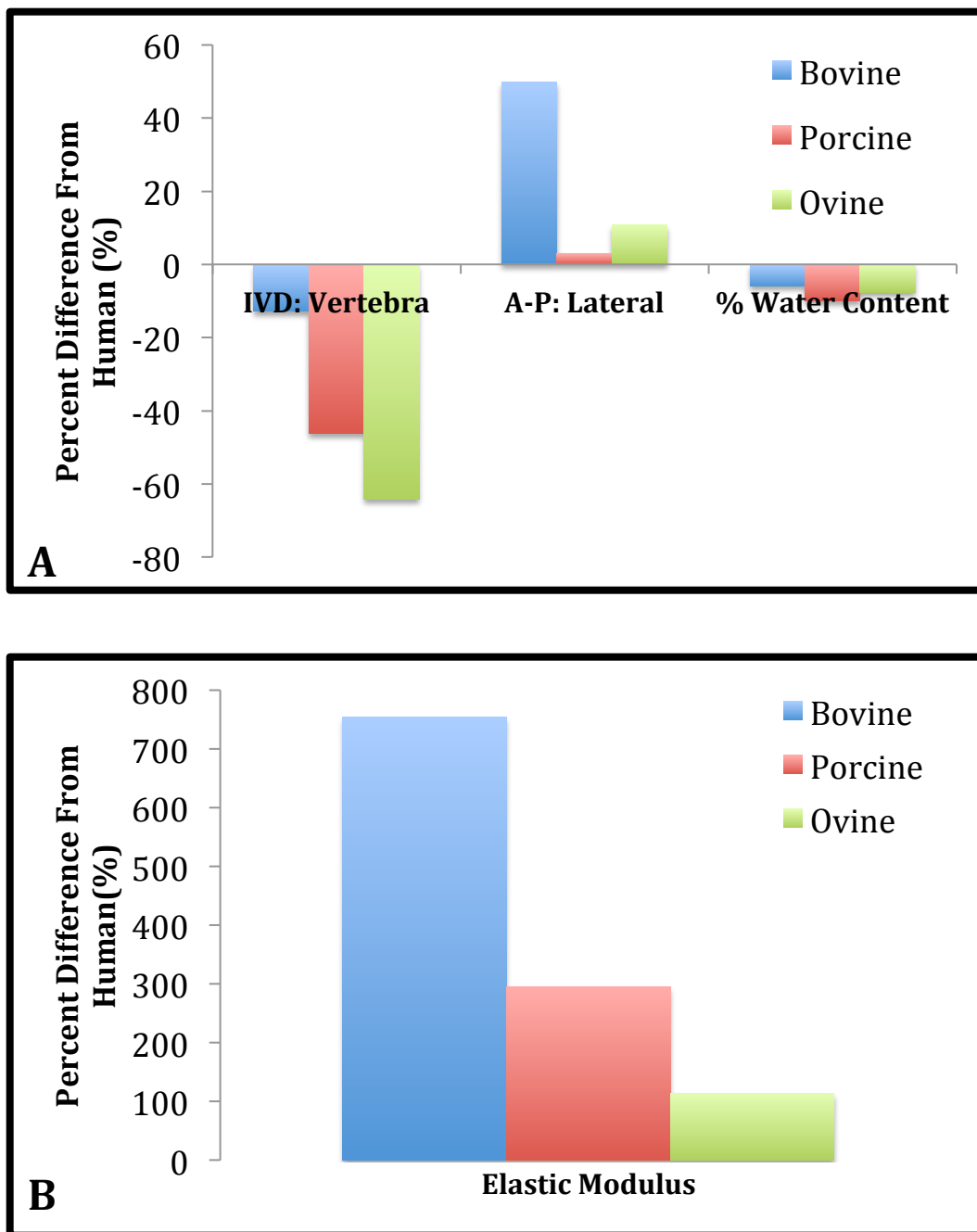
Figure 30. Graphical representation of percent difference values of bovine tail, porcine lumbar, and ovine lumbar intervertebral disc properties from human lumbar intervertebral disc (IVD) for (A) [1]intervertebral disc: vertebral height, [2]anterior-posterior (A-P): lateral width ratios, [2]water content (%), and (B) [3]elastic modulus. Human values calculated from [1]Busscher et al. (2010), [2]Beckstein et al. (2008), and [3]Holzapfel et al. (2005).

Chapter 4:

Discussions

This project compared the biomechanical, geometric, hydration, and histological properties between commonly used models species in IVD research. It was found that the bovine and ovine models differed the most from one another for most properties and the porcine model was the most intermediate model.

Examining the geometry, water content, and histology is critical as each contribute to the biomechanics of the IVD. IVD and vertebral geometry play a role in distributing forces throughout the IVD, which influences the internal hydrostatic pressure within the NP. This internal swelling pressure is regulated by the amount of water within the NP, which is, in turn, affected by ECM proteins. Both compressive forces and osmotic diffusion of water through the vertebral endplate regulate the amount of water in the IVD (Ohshima et al., 1989). The compressive and tensile strength of the IVD is determined by the abundance and presence of collagen and proteoglycans within the AF and NP (Hayes et al., 2001; Errington et al., 1998; McNeilly et al., 1996). The cells of the IVD produce these ECM structures and the output of these cells is influenced by biomechanical changes (i.e. compressive and tensile forces) in the matrix (Oegema, 1993). Together, geometry, water content, and histology regulate and determine the biomechanics of the IVD, but also act to regulate one another.

Although animal models and human spines are morphologically different *in vivo* (eg. humans have 5 lumbar vertebrae, whereas porcine and ovine have 6-7 vertebrae; bovine tail vertebrae have less boney posterior elements than the human vertebrae), a comparison between quadrupeds and bipeds can be conducted. This is due to the fact that the majority of the forces acting on the IVD in both the models and humans are derived from the surrounding spinal musculature (eg. psoas major, erector spinae, and multifidus). A comparative analysis of the

properties of the model and human IVDs can therefore be conducted with little consequence of *in vivo* locomotion.

4.1 Anatomy

4.1.1 Geometry

Height and width ratio differences between models observed in this study suggest that each model has unique anatomical proportions. These differences are likely due to anatomical adaptations as a result of varying internal forces (i.e. from surrounding muscles and tendons), which are due to the physical location of the IVDs (tail versus lumbar spine region). This study found that the bovine specimens had the highest IVD: vertebral ratios while the ovine had the lowest. This supports the first hypothesis that the size and shape of bovine tail IVD would differ the most from the porcine and ovine IVDs. Further, these differences were due to different sized IVDs ($p < 0.01$) rather than vertebral heights ($p > 0.05$). Specifically, the bovine IVDs were much taller in comparison to both the porcine and ovine IVDs. Since the ovine had the smallest IVD ratio (0.14; table 11) and thus smaller IVD height, under similar axial loading conditions the ovine IVD would deform differently and potentially experience more axial strain than the bovine tail, which had a larger height ratio (0.34; Figure 20). Interestingly, the bovine IVD: vertebral height ratio (Table 11) was most similar to humans, which had a ratio of 0.39 (calculated from Busscher et al., 2010). The bovine height ratio had a lower percent difference (12.8%) from the human, in comparison to porcine (46.15%) and ovine (64.1%) (Figure 30).

The higher ratio exhibited by the bovine specimens has possibly adapted in nature to allow more movement in the tail (primarily bending, i.e. swinging tail to brush off flies) as compared to the lumbar region of the other models. The lumbar region of the ovine and porcine

may not have the same movement capabilities as the human lumbar spine, which may explain why bovine IVD: vertebral heights most closely resembled human. Given the different IVD: vertebral height ratios for all three species, and in particular the ovine and porcine, caution needs to be exercised when examining full joint mechanics. For example, a herniation of the NP has been successfully induced *in vitro* by repetitively bending a functional spine joint under moderate compressive load (Callaghan & McGill, 2001, Tampier et al., 2007, Gregory & Callaghan, 2011). If an ovine or porcine specimen were to be used, the force applied to bend the segment would need to be adjusted to generate a similar bending moment or an altered mechanism of injury could result.

Similar to the IVD: vertebral heights, the A-P: lateral width ratios differed between the three specimens. These differences are visually quite clear in the transverse sectioned samples (Figure 1). A width ratio greater or less than 1.0 would suggest that a particular width is larger in one direction than in the other, whereas a width ratio of ~1.0 would suggest a relatively circular shape. The gross anatomy of the model IVDs revealed that the bovine tail is more circular in shape (ratio: 1.01 ± 0.09), whereas the other two models are more wide than deep (porcine ratio: 0.66 ± 0.036; ovine ratio: 0.74 ± 0.06). This supports the first hypothesis that the bovine tail would differ the most geometrically from the other models. The overall shape and width ratio of the porcine and ovine IVD more closely resembles that of the human IVD (2.94%, 8.12% difference from humans, respectively; Figure 30), which has a width ratio of approximately 0.68 (calculated from Beckstein et al., 2008). The bovine differed the most from humans for width ratio (48.53% difference; Figure 30).

Similar to the height ratios, transverse shape differences would have implications on the distribution of forces throughout the IVD. Since both A-P and lateral widths are nearly equal in

the bovine IVD, the annulus would likely experience similar radial forces from the NP on both the A-P and lateral walls. This is different from the human annulus where different regions experience different loads (McNally & Adams, 1992). Even with similar hydrostatic pressure within the NP of the three models, the different A-P and lateral ratios would alter how this pressure is transferred to the annulus and thus how these forces are dissipated throughout the IVD. Therefore the bovine IVD may not be the most appropriate model for whole IVD mechanics.

Overall, the average IVD heights and lateral and A-P widths were consistent with previous literature examining animal models (Beckstein et al., 2008; O'Connell et al., 2007) (Table 4).

4.1.2 Water Content

An unexpected finding was that the normalized whole IVD water content did not differ between species, which failed to support the first hypothesis that the porcine would have the highest water content. A visual comparison of the porcine IVD with the other models revealed that the NP appeared more liquid than the other models. This led to the initial hypothesis that the porcine had the greatest water content of all three models. The porcine has an undoubtedly high water within the NP, which leads to the conclusion that the AF must have a lower water content than the AF of the other models as the whole IVD water content was not significantly different. A study by Beckstein et al. (2008) compared region-specific water percent content of the bovine tail, porcine lumbar, and ovine lumbar for the outer AF, inner AF, NP. Although statistical comparisons were not conducted between the three models in Beckstein et al (2008) (they were compared individually to the human IVD), there did not appear to be a significant trend for higher water content in the porcine NP compared to the other models. However, unlike the

protocol for this project, the study by Beckstein et al. (2008) did not normalize the water content data to take into account IVD weight. It is possible that region-specific water content normalized to sample weight would reveal differences in the porcine compared to the ovine and bovine.

This study found that the percent water content of the bovine IVD differed the least (5.83%; Figure 30) from human percent water content (77.67%; Beckstein et al., 2008). The porcine had the highest percent difference from humans (9.99%) and the ovine had intermediate percent difference (7.57%) between the other models. The water content (%) values calculated in this project (Table 11) were consistent with values calculated from Beckstein et al (2008). However, this project found that the ovine had the most intermediate water content (71.79%, versus 73.14% for bovine and 69.91% for porcine), whereas the values from Beckstein et al. suggest that the porcine model had the most intermediate water content (70.33% versus 76.67% for bovine and 66% for ovine; Table 4). However, since no significant differences were observed in water content across the three species, no species is a more appropriate model for the human IVD than another.

4.2 Tensile Properties

The tensile properties of the lamellae from animal models are important characteristics to consider as they can give insight to the progression IVD disorders and diseases. The overall result was that the porcine was the intermediate model and deviated the least from the bovine and ovine species. It was found that bovine tail deviated the most from the other two models, especially from the ovine lumbar. This finding supports the second hypothesis that models, which differ the most from one another geometrically, will exhibit significantly different tensile properties.

The biomechanical differences in the bovine tail can, in part, be explained by the fact that the bovine IVD was extracted from the tail and not the lumbar region. In general, the bovine AF samples were found to be stiffer, reach higher stresses and deform less in comparison to the porcine and ovine samples. In contrast, the ovine samples were found to be more compliant, reach lower stresses and deform more. *In vivo*, a tail undergoes different biomechanical loads and has different movement requirements due to its anatomy. For instance, musculature within the tail is reduced distally, and becomes increasingly tendinous. Near the base of the tail, the muscular forces generated in the erector spinae muscle of the back are transferred to the IVD by tendons located very close to the joint (Young & Kenrick, 1989) rather than by muscles acting further from the IVD as in the case for the ovine spine (Keller et al., 2007). The bovine tail IVD may have adapted to these force differences resulting in a stiffer AF. Additionally, the tail does not likely undergo axial rotation unlike the lumbar spine which can go through substantial rotation in the human depending on the body's activity (3-49°; Bible et al, 2010) and the IVD may have also adapted to this by resulting in a stiffer AF tissue. Compared to the elastic modulus of human tissues (0.22; Holzapfel et al, 2005), the models exhibited higher stiffness values and ultimately high percent differences from human values (bovine: 754%; porcine: 295.5%; ovine: 113.6%; Figure 30).

In comparison to the previous studies that examined single layers of the AF from a bovine tail model, the bovine specimens in this study reached higher initial failure stresses than those in Pezowicz et al. (2005) (0.15 MPa as compared to 0.50 MPa). However, due to tissue extraction techniques and sample mounting (in the mechanical system), the samples tested by Pezowicz et al. did not show the traditional stress-strain relationship of soft tissues and did not

appear to have a classic initial point of failure shown in Figure 6. As a result, the tissues in this study seemed to reach higher stresses prior to any signs of failure.

The strain properties of the porcine AF found in this study (Table 10) were similar to the values found in Gregory & Callaghan (2011), however there were substantial differences in the stress values. This project found the toe-region, initial, failure, and ultimate failure stress values to be 0.09 MPa, 0.50 MPa, and 0.77 MPa, respectively. In Gregory & Callaghan (2012) stress values were higher for toe-region (0.33 MPa), initial failure (1.09 MPa), and ultimate failure (failure strength; 1.44 MPa). However, these values were for specimens from the cervical spine that had undergone a two-hour loading protocol, while the specimens in this study were from the lumbar region and did not undergo any loading protocol.

4.3 Histology: Extracellular Matrix Proteins and Cells

The tensile properties of bovine tail and the ovine lumbar IVD differed the most from one another in stress and strain values, and the elastic modulus of the bovine tail differed the most from both the porcine and ovine lumbar. Similarly, the bovine histology differed the most from the other models in that it had the lowest cell content in the inner AF and NP, highest cell count in the outer AF, and a higher proportion of proteoglycans in the inner AF. These findings support the second and third hypotheses that models with similar proportion and distribution of ECM structures will exhibit similar tensile properties.

The overall distribution of collagen and proteoglycan was not different between species (i.e. collagen type I was found in the outer AF, collagen type II was found in the IAF and NP, and proteoglycans were found in the inner AF and NP). This finding makes sense because each component of the IVD (outer AF, inner AF, and NP) is designed to function in a particular way

and does so because of the tensile or compressive strength properties of collagen types I and II, and proteoglycans. The compressive strength of the NP and the tensile properties of the IVD are important in maintaining the integrity of the IVD and have thus been preserved in all three species.

It was hypothesized that the porcine IVD would have higher proteoglycan content in the NP, and the results from this work support this hypothesis. The NP of the porcine was primarily saturated with proteoglycans and very little collagen. This leads to a less collagenous and fibrous and a more liquid NP. While this wasn't emulated in a difference in IVD water content, it does support the appearance of a more liquid NP in the porcine IVD.

An unexpected finding was that proteoglycans were present in higher amounts in inner AF of the bovine tail than the other models (Figure 27), especially in the transition zone between the outer AF and inner AF. This finding can be confirmed by Beckstein et al. (2008) who found that the sulfated-GAG content in the inner AF was higher in the bovine tail than porcine and ovine lumbar IVDs (Table 5). Specifically, it was found that the sulfated-GAG content of the inner AF in the bovine tail was 394 ± 172 μg/ mg, whereas the inner AF of the porcine and ovine had sulfated-GAG contents of 150 ± 19.7 μg/ mg and 260 ± 55.5 μg/ mg (Table 5). The sulfated-GAG content of the human inner AF (377 ± 185 μg/ mg) was significantly more than the sulfated-GAG content in the porcine or ovine, but was similar to the inner AF of the bovine (Table 5). The higher sulfated-GAG content in the bovine tail may be explained by the presence of proteoglycans in the more medial layers of the inner AF (further away from the NP) than in the other models.

A greater elastic modulus of the bovine tail can additionally be explained by a higher collagen content in the inner AF. Histologically, it was found that collagen type I persisted in

AF layers closer to the NP in the bovine compared to the other models (Figure 28). Increased

collagen in the inner AF has also been observed by Showalter et al (2012). Showalter et al.

(2012) found that the inner AF of the bovine tail had a collagen content of 43.4 ± 18 μg/ mg dry

weight, whereas the porcine and ovine models had a collagen content of 5.8 ± 2.9 μg/ mg and 9.2

± 10.6 μg/ mg, respectively (Table 5). Therefore, this increased collagen may explain the higher

elastic modulus observed in the bovine model.

The most prominent histological difference between species was the presence and

concentration of cell types throughout the IVD. The ovine IVD had the highest overall

concentration of cells in the inner AF and NP, and had an exceptionally high concentration of

notochordal cells within the NP (Figures 22 and 23). This high concentration of cells in both the

porcine and ovine may be explained by differences in nutritional supply from the vertebral body

to the IVD and the permeability of the vertebral endplate between species. Several factors,

including calcification (Roberts et al., 1996; Urban et al., 2004), create a nutritional barrier

between the blood supply of the vertebral body and the IVD. Since the IVD is mostly

unvascularized, any nutrients supplied to the IVD must be obtained from the vascularized

vertebral body via transport through the vertebral endplate. Blocking or decreasing the vertebral

endplate permeability causes a slower diffusion of solutes (Roberts et al., 1996), and prevents the

IVD from receiving a sufficient amount of solutes to supply the cells. Given that cell viability is

dependent on nutrient levels (Bibby et al., 2002), and that NC cells have been shown to have a

high nutritional demand (Guehring et al., 2010), one would expect to see a higher viability of NC

cells in IVDs with a higher nutritional supply. The porcine and ovine may have a more

permeable (less calcified, for example) vertebral endplate than the vertebral endplate of the either

bovine or porcine models. This may explain the high concentration of cells, especially NC,

within the ovine IVD, however species-specific vertebral endplate permeability has not been documented in the literature. Further research must be conducted to explore the differences in composition of the vertebral endplate between the three models.

As CCL and NC primarily produce collagen type II and proteoglycans (respectively), it would be expected that the collagen and proteoglycan contents within the ovine NP would be the greatest in this model. However, this was not the case (Table 5). In contrast, the bovine tail had the lowest concentration of cells throughout the inner AF and NP, yet had a visually higher amount of both proteins (Table 5).

Another unexpected result was that NC were detected in the NP of all species. In older individuals and skeletally mature animals, NC are thought to be lost and replaced with CCL, therefore it would be expected that the models would be fairly devoid of NC. However, a study conducted by Trout et al. (1982) found the presence of NC in human IVDs from 8 weeks of age to 32 years. Given the presence of NC, these models may more appropriately represent young healthy adult IVDs; Table 12 describes the age equivalence of the models based on the lifespan of the animal.

4.4 A Model for Humans

4.4.1 Bovine Model

The geometry of the bovine IVD is both similar and dissimilar to the human IVD. Specifically, the A-P: lateral width ratio deviated the most from human data (48.53%; Figure 30), however, the IVD: vertebral height ratio deviated the least (12.8%; Figure 30). Full joint mechanics, or FSU mechanics, may be most suitable in the bovine model, especially regarding

Table 12. Age equivalence in human years of bovine, porcine, and ovine models based on typical age at slaughter.

Species	Life Expectancy (years)	Average age of Slaughter (years)	"Human" Age (years)
Cow	15	2-3	16
Pig	8	2	20
Sheep	10-12	4	26

studies of low back disorder progression, such as herniation. As the bovine deviated the least from the human IVD: vertebral height ratio, this suggests that the bovine tail FSU has similar bending mechanics to the human FSU. This similarity suggests that similar mechanisms of FSU injury may progress in the bovine tail *in vitro* as a human FSU *in vitro*.

Given that the bovine A-P: lateral width deviated the most from human IVD, it may not be the most appropriate model for full IVD mechanics. The transfer of forces within a more circular IVD, such as the bovine tail, is different than in a limacon IVD, such as in the human lumbar, because the pressurization of the NP would differ, and thus affect how forces are transferred radially to the AF. Additionally, the biomechanics of the bovine tail, specifically the elastic modulus, differed the most from humans (754% deviation; Figure 30) and would be the least appropriate model for tissue mechanics.

4.4.2 Porcine Model

The porcine model was the most similar to humans in AP: lateral width geometry (2.94% difference), which would suggest that it is the most appropriate model for whole IVD mechanics. However, whole IVD water content differed the most from humans (9.99%), which would have an effect on how the forces in the NP are transferred to the AF. As water content did not significantly differ between models, the higher percent deviation of the porcine model from the human may not be a significant factor. However, caution must be taken when using the porcine for whole IVD mechanics as the consistency of the NP is more liquid, which may affect force distribution throughout the IVD.

4.4.3 Ovine Model

The mechanical properties of ovine AF deviated the least from the human (elastic modulus: 113.6%). This would suggest that the ovine would be the most appropriate model for

isolated tissue mechanics (compared to over 700% deviation between bovine and human), however this is still a substantial deviation. The AP: lateral width deviated slightly more from the human than the porcine model (8.12%) but may also be an appropriate model to consider for whole IVD mechanics as this deviation was not exceptionally large.

However, if full joint mechanics are considered, the ovine FSU would be the least appropriate model to represent human FSU mechanics. The IVD: vertebral ratio of the ovine had the highest percent deviation from humans (64.1%). This suggests that the ovine FSU likely exhibits different bending mechanics compared to the human FSU.

4.4.4 Model Conclusions

For each property measured, a different model was closer in value to the values of the human IVD properties (Table 13), which supports the fourth hypothesis that some models will be closer in value to human values than others. Due to this, a single model cannot be used for all applications of IVD testing (eg. isolated tissue mechanics, joint mechanics, whole IVD mechanics) and a different model must be chosen for testing depending on the application of the research. The bovine and porcine models would best represent the human for whole joint and full IVD mechanics, such as forward flexion-extension tests to induce herniation or testing the effect of vibration on the formation of clefts in the AF, due to their close resemblance to human geometry. Lastly, the ovine model would best represent human AF tissue mechanics, such as studying the effects of compressive load on the tensile strength of the lamellae.

Table 13. Percent deviation of intervertebral disc (IVD) of model species from human "gold standard" values for elastic modulus, IVD: vertebral height ratio, and anterior-posterior (A-P): lateral width ratio, and the application of models for use in human research. Human values obtained from [1]Holzapfel et al. (2005), [2]Busscher et al. (2010), and [2]Beckstein et al. (2008). Italicized species names represents model closest in value to human "gold standards"; standard deviation reported.

Properties Measured	Human "Gold Standard" Values	Model Values	Percent Deviation from Human	Type of Test	Example Application of Research
Elastic Modulus	0.22 ± 0.2 MPa	Bovine: 1.88 ± 1.26 Porcine: 0.78 ± 0.61 *Ovine: 0.47 ± 0.38*	Bovine: 755% Porcine: 296% *Ovine: 114%*	Tissue mechanics	Determining if the tensile strength of the annulus fibrosus is affected by perturbations in the external environment such as axial loading
IVD: vertebral height ratio	0.39	*Bovine: 0.34* Porcine: 0.21 Ovine: 0.14	*Bovine: -13%* Porcine: -46% Ovine: -64%	Full joint, functional spine unit mechanics	Testing the progression of intervertebral disc herniation through forward flexion/ extension of full joint, which is known to induce herniation
A-P: lateral width Ratio	0.68	Bovine: 1.01 *Porcine: 0.66* Ovine: 0.74	Bovine: 49% *Porcine: 3%* Ovine: 8%	Whole IVD mechanics	Determining the effect of vibration on the integrity of the IVD

Chapter 5:

Conclusions

5.1 General Conclusions

The three models analyzed in this study showed marked differences in biomechanical, geometric, and histological properties between one another. As a result, one species may be more appropriate as a model for the human IVD for a particular application while a different species is more appropriate for another application (i.e. a model may be more suitable for tensile testing, but may not be the most suitable model to test cellular response mechanisms). Therefore, an appropriate model must be carefully chosen depending on the objective of research question.

Overall, the porcine model remained the model intermediate between the three species and was not significantly different from either model in most areas of comparison. The bovine model displayed the largest deviation from the other models most likely due to its source location (tail rather than lumbar spine).

Although a single definitive model for human studies cannot be determined at this stage in the project, it can be concluded that each model has unique properties that can represent different components of the human IVD. It was found that the bovine had the most similar height ratio to the human and would therefore be the most appropriate model to represent human full joint mechanics. The porcine model was found to be the most appropriate model for whole IVD mechanics, such as studying the effect of vibration on the integrity of the AF, as the A-P: lateral width measurements deviated the least from humans. Lastly, the ovine elastic was closest in magnitude to values for the human AF in the literature suggesting that this model is the most appropriate for AF mechanical testing, such as determining the tensile strength of a tissue under conditions known to induce low back disorders.

The most substantial contribution to the literature that this work has provided is the comparison of the single layer AF tissue mechanics of the three species. Comparing single

lamellae of the AF compares the most basic biomechanical element of the IVD (Skaggs et al., 1994), which, in turn, compares the biomechanical foundation of each species with one another. Much like bricks in house, the overall strength of the IVD is determined by the interaction of the smallest unit, which, in the IVD, can be analogous to the individual collagen fibres of the AF lamellae. If the bricks of the house are damaged, the overall integrity of the house is challenged, as is the case for low back disorders, such as herniation or prolapse, which can develop from weaknesses in the AF. Therefore, the data collected in this study will help determine an appropriate model for IVD research and contribute to our understanding of injuries to the spine and IVD. Further, the basic material properties determined for the AF for each of these species can be also used in the development of IVD models (eg. finite element models).

Although animal models may have their limitations (Alini et al., 2008; Demers et al., 2004), the scarcity of healthy human tissue and the lack of ability to control for factors *in vivo* make animal models indispensable in IVD and spine research (Smith et al., 2011). By studying the characteristics of these models researchers can manipulate tissues in ways that represent real forces *in vivo* in a controlled environment. Insight can be gained into the functioning of the human spine and used to better predict factors that lead to the progressing of low back disorders.

5.2 Novel Findings

This study was unique in that it is one of the first studies to determine various tensile properties of single layer AF tissues perpendicular to their fibre orientation for animal models. Data from this project will not only contribute to a better understanding of the mechanical properties of models, but will also highlight the similarities and differences between model species and humans. Additionally, studying the mechanics of the tissue in this orientation can

help researchers understand the progression of low back disorders, such as herniation, and how the IVD may fail.

Normalizing variables, such as water content, compared models on the same scale and revealed whether differences or similarities seen were due to size or the inherent properties of the tissue. This led to a more effectual comparison of results between the models. For example, this project normalized water content by IVD weight and revealed that there were no differences between species. This novel finding contradicts the hypothesis that the porcine model has higher water content due to a more liquid NP, and reveals that there may be other factors that contribute to the morphology of the porcine NP.

It was further hypothesized that the liquid NP was due to higher cell content within the porcine NP, but our findings reveal that the porcine and ovine models had the highest and most similar cell count. This unexpected finding suggests that there are more inherent differences between models that attribute to their properties. Additionally, the use of histology to explain differences seen in biomechanical properties of single AF lamellae is a novel approach. Most studies compare the content of cells and ECM proteins for the components of the IVD (AF, NP), but do not consider the fundamental structure of the IVD. It was found that the qualitative and quantitative cell and ECM characteristics correlated with the biomechanical properties of single lamellae. For instance, the higher tensile strengths and elastic modulus of the bovine tail was reflected in the fact that the bovine model had a larger area of collagen type I in the outer AF, and a higher cell count in the outer AF.

5.3 Considerations

This study was limited in that the tissues used were extracted from animals post mortem. Post mortem tissue testing may have had an effect on the reported biomechanical values, as tissues were not in the same physiological environment as they would have been when the animal was alive. *In vivo*, tissues are more hydrated and living cells are producing proteins and other structures. The homeostatic environment of the living body would regulate ions and other biological factors, which may impact the biomechanics of the tissue. While freezing is a limitation, it is not expected to have a large effect on the results of this work as it has been previously shown to have little effect on tissue biomechanics (Dhillon et al., 2001; Callaghan & McGill, 1995). In addition, it has been shown that different levels of post mortem hydration can affect tissue swelling and thus stiffness of the AF layers (Gruevski et al., 2014). However, differences observed between species would not have likely been affected as all tissues were exposed to the same testing environment prior to and during testing.

Another consideration of this project was that AF samples for mechanical testing were primarily extracted from the more superficial layers of the AF. It has been shown that the biomechanical properties varying depending on the region of IVD that is tested (Skaggs et al., 1994), especially between the outer AF and inner AF, and it would have been therefore beneficial to compare the more superficial and deeper layers of the AF. Due to difficulties during dissection and testing, obtaining tissues from the inner AF was challenging. Additionally, comparing the water content of the AF and NP separately may have revealed an explanation as to why whole IVD water content was statistically insignificant (i.e. the porcine NP may have had a higher water content and AF may have a lower water content than the other models).

Lastly, data were only compared to previously published human values. A direct comparison using the same methods would have been ideal but was not possible as it was beyond the scope of the current project.

5.4 Future Directions

Further research should focus on incorporating and comparing human tensile data with the model data to determine which model would be most suitable for IVD studies. This would provide researchers with a "model manual" to help choose the appropriate animal model for future studies. Further, a more thorough cell and ECM analysis using immunostaining and assays would help identify and quantify these structures. Lastly, a comparison of the anatomy of the vertebral endplate of the three models would be beneficial to understand if differences in cell densities could be due to differences in nutritional supply from the vertebral bodies. Measurements of permeability can be conducted by measuring the relaxation pressure caused by the transient-flow rate of fluid into the IVD, as outline in Accadbled et al. (2008).

5.5 An Integrative Approach to IVD Research

The human body is a complex set of tissues and organs that work harmoniously together to maintain homeostasis within the body. Each individual component of the body (cells, tissues, organs, etc.) maintains equilibrium in a unique matter that, when combined, function as a whole. The IVD is no exception and maintains its own balance through the use of specialized cells, proteins, and ECM structures. The study of IVDs cannot be achieved by looking through a single scientific lens. The tissue itself functions mainly as a biomechanical structure. However, its ability to allow flexibility and maintain stability of the spine is influenced by the biochemical

and anatomical properties it possesses. Thus integration of various scientific fields, including biology, biochemistry, cell biology, kinesiology, engineering, and biomedical sciences, must be considered when studying the IVD (Figure 31). Further, other fields, including sociology, and psychology must also be considered when studying the complexities of low back disorders.

Low back disorders are one of the most common musculoskeletal disorders in North America and the leading cause of disability amongst workers worldwide (Buchbinder et al., 2013). Spine injuries such as damage to the IVD can cause substantial pain and lead to lost productivity in the workplace and a substantial cost to the healthcare system. Given the substantial impact that low back disorders have on society, IVD research is not only a matter of scientific enhancement, but also a solution to a bigger social problem. Discovering an adequate animal model for IVD research will allow researchers to obtain valuable data from tissues that are more accessible. More data on IVD will accelerate the development of novel therapeutic and rehabilitative techniques for low back disorders, which can improve the lives of individuals suffering from these ailments.

This project not only incorporated background knowledge from other fields of research, but also utilized techniques and equipment used in other fields of research. For instance, the BioTester 5000 used in this project has been designed to study the tensile properties of biological soft tissues. However, this system can be further used to test synthetic biomaterials and tissue scaffolds. Biomechanics is very closely related to bioengineering in that rehabilitative biotechnology must mimic the biomechanics of the body.

The biomechanics of the IVD cannot be fully understood without looking at the biological factors that influence these properties. Histological staining is a common practice in
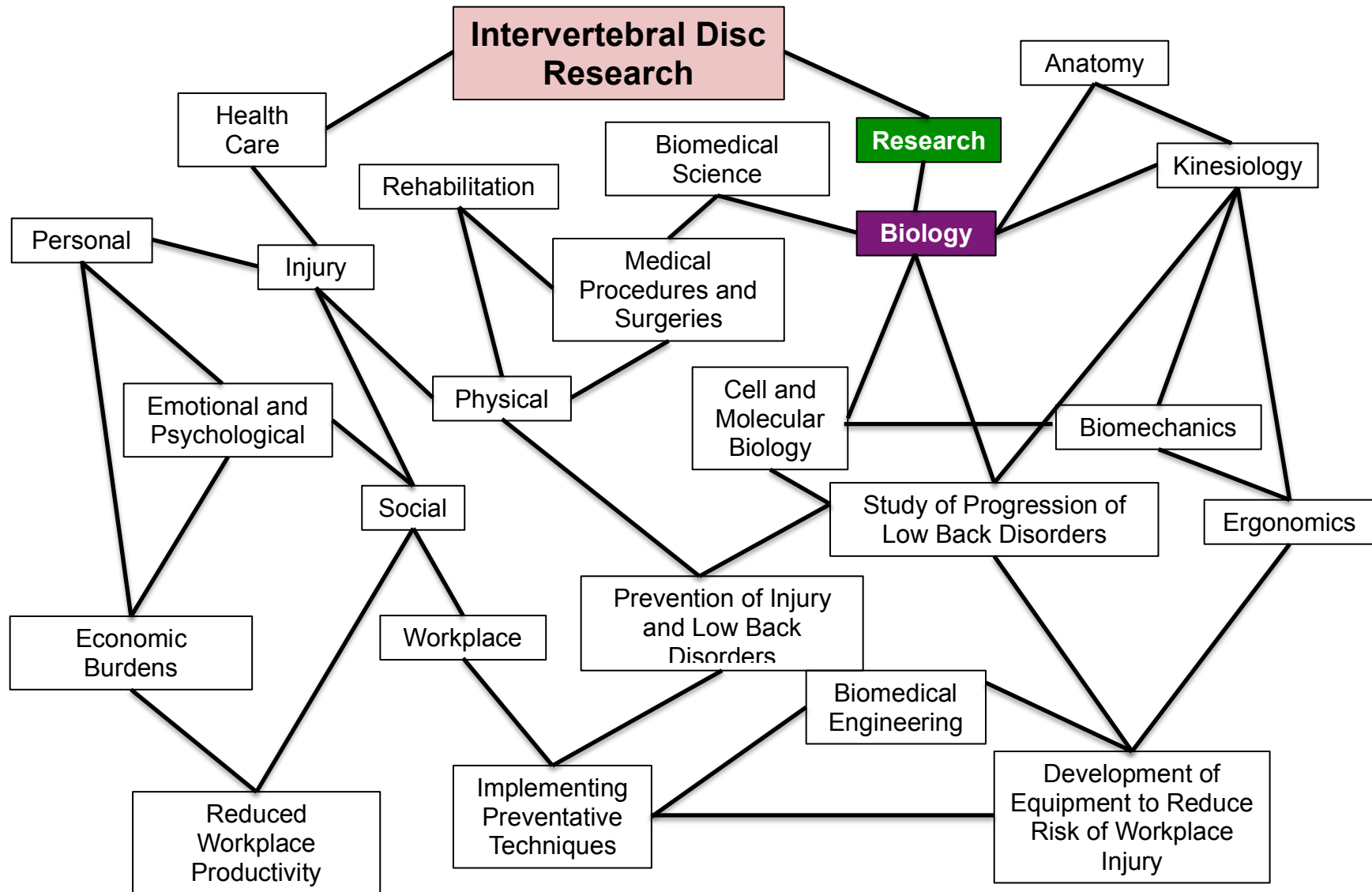
Figure 31. Schematic showing an integrative approach to intervertebral disc research. The project integrates research biology with numerous fields and applications of research.

human and veterinary medicine as a diagnostic tool to verify the presence of cells, proteins, pathogens, or other structures. Similar techniques were integrated into the data analysis of this project to verify the presence of cellular and ECM structures and understand the biomechanical properties of the IVD. Although the objectives of using histological techniques in this project were not diagnostic the results obtained helped to explain the biomechanical differences seen between species.

Integrating background knowledge and technologies from different fields of research allows researchers to study the IVD from different perspectives and helps to improve our understanding on the complexity and multifactorial nature of low back disorders and IVD health.

Literature Cited

Accadbled, F., Ambard, D., de Gauzy, J.S., and Swider, P. (2008). A measurement technique to evaluate the macroscopic permeability of the vertebral end-plate. *Journal of Medical Engineering and Physics*, 30(1): 116-122

Adams, P., Eyre, D.R., and Muir, H. (1977). Biochemical aspects of development and ageing of human lumbar intervertebral disc. *Rheumatology and Rehabilitation,* 16: 22-29.

Adams, M.A., and Dolan, P. (1995). Recent advances in lumbar spinal mechanics and their clinical significance. *Clinical Biomechanics*, 10(1): 3-19.

Adams, M.A., McNally, D.S., and Dolan, P. (1996). 'Stress' distribution inside intervertebral discs: The effects of age and degeneration. *The Journal of Bone and Joint Surgery*, 78-B(6): 965-972.

Adams, M., Bogduk, N., Burton, K., and Dolan, P. (2006). *The Biomechanics of Back Pain*. (2nd ed.). Phi1adelphia (PA): Elsevier Churchill Livingstone.

Aguiar, D.J., Johnson, S.L., Oegema, T.R. (1999). Notchordal cells interact with nucleus pulposus cells: Regulation of proteoglycan synthesis. *Experimental Cell Research,* 246: 129-137.

Antoniou, J., Steffen, T., Nelson, F., Winterbotoom, N., Hollander, A.P., Poor, R.A., Aebi, M., and Alini, M. (1996). The human lumbar intervertebral disc: Evidence for changes in the biosynthesis and denaturation of the extracellular matrix with growth, maturation, ageing, and degeneration. *Journal of Clinical Investigation,* 98(4): 996-1003.

Beckstein, J.C., Sen, S., Schaer, T.P., Vresilovic, E.J., and Elliott, D.M. (2008). Comparison of animal discs used in disc research to human lumbar disc. *Spine*, 33(6): E166-E173.

Berthet-Colominas, C., Miller, A., Herbage, D., Ronziere, M-C., and Tocchetti, D. (1982). Structural studies of collagen fibres from intervertebral disc. *Biochimica et Biophysica Acta,* 706: 50-54.

Bibby, S.R.S., Fairbank, J.C.T., Urban, M.R., and Urban, J.P.G. (2002). Cell viability in scoliotic discs in relation to disc deformity and nutrient levels. *Spine*, 27(20): 2220-2228.

Bible, J.E., Biswas, D., Miller, C.P., Whang, P.G., and Grauer, J.N. (2010). Normal functional range of motion of the lumbar spine during 15 activities of daily living. *Journal of Spinal Disorders and Techniques*, 23(2): 106-112.

Bron, J.L., Helder, M.N., Meisel, H-J., Van Royen, B.J., and Smit, T.H. (2009). Repair, regeneration and supportive therapies of the annulus fibrosus: achievements and challenges. *European Spine Journal,* 18: 301-313.

Brown, S.H.M., Gregory, D.E., Carr, J.A., Ward, S.R., Masuda, K., and Lieber, R.L. (2011). Adaptations to the multifidis muscle in response to experimentally induced intervertebral disc degeneration. *Spine,* 36(21): 1728-1736.

Bruehlmann, S.B., Rattner, J.B., Matyas, J.R., Duncan, N.A. Regional variations in the cellular matrix of the annulus fibrosus of the intervertebral disc. *Journal of Anatomy,* 201: 159-171.

Buchbinder, R., Blyth, F.M., March, L.M., Brooks, P., Woolf, A.D., and Hoy, D.G. (2013). Placing the global burden of low back pain in context. *Best Practice and Research Clinical Rheumatology*, 27: 575-589.

Busscher, I., Ploegmakers, J.J.W., Verkerke, G.J., and Veldhuizen, A.G. (2010). Comparative anatomical dimensions of the complete human and porcine spine. *European Spine Journal*, 19: 1104-1114.

Callaghan, J.P., and McGill, S.M. (1995). Frozen storage increases the ultimate compressive load of porcine vertebrae. *Journal of Orthopaedic Research*, 13: 809-812.

Callaghan, J.P., and McGill, S. (2001). Intervertebral disc herniation: studies on a porcine model exposed to highly repetitive flexion/extension motion with compressive force. *Clinical Biomechanics*, 16: 28-37.

Cassidy, J.J., Hiltner, A., and Baer, E. (1989). Hierarchical structure if the intervertebral disc. *Connective Tissue Research,* 23: 75-88.

Chelberg, M.K., Banks, G.M., Geiger, D.F., and Oegema, Y.R. (1995). Identification of heterogeneous cell populations in normal human intervertebral disc. *Journal of Anatomy*, 186(1): 43-53.

Chou, A.I., Bansal, A., Miller, G.J., and Nicoll, S.B. (2006). The effect of serial monolayer passaging on the collagen expression profile of outer and inner anulus fibrosus cells. *Spine,* 31(17): 1875-1881.

Demers, C.N., Antoniou, J., and Mwale, F. (2004). Value and limitations of using the bovine tails as a model for the human lumbar spine. *Spine*, 29(24): 2793-2799.

Dhillon, N., Bass, E.C., Lotz, J.C. (2001). Effect of frozen storage on the creep behavior of human intervertebral discs. *Spine*, 26: 883-888.

Doita, M., Kanatani, T., Harada, T., and Mizuno, K. (1996). Immunohistologic study of the ruptured intervertebral disc of the lumbar spine. *Spine*, 21(2): 325-241.

Errington RJ, Puustjarvi K, White IR, Roberts S, Urban JP. (1998). Characterisation of cytoplasm-filled processes in cells of the intervertebral disc. *Journal of Anatomy,* 192: 369–378.

Ghosh, P., Taylor, T.K.F., Braund, K.G., and Larsen, L.H. (1976). A comparative chemical and histochemical study of the chondrodystrophoid and nonchondrodystrophoid canine intervertebral disc. *Veterinary Pathology,* 13: 414-427.

Gower, W.E. & Pedrini, V. Age-related variations in protein-polysaccharide from human nucleus pulposus, annulus fibrosus and costal cartilage. *Journal of Bone and Joint Surgery,* 51(A): 1154-1162.

Gregory, D. E. & Callaghan, J.P. (2011). Does vibration influence the initiation of intervertebral disc herniation? *Spine,* 36(4): 225-236.

Gregory, D.E. & Callaghan, J.P. (2012). An examination of the mechanical properties of the annulus fibrosus: The effect of vibration on the intra-lamellar matrix strength. *Medical Engineering and Physics,* 34: 472-477.

Gregory, D.E., Bae, W.C., Sah, R.L., and Masuda, K. (2014). Disc degeneration reduces the delamination strength of the annulus fibrosus in the rabbit annular disc puncture model. *Spine*, 14(7): 1265-1271.

Gruber, H.E., Ingram, J, and Hanlet, E.N. Jr. Ingram, J**. (**2002). An improved staining method for intervertebral disc tissue. *Biotechnic and Histochemistry***,** 77(2): 81-83.

Gruevski, K.M., Gooyers, C.E., Karakolis, T., and Callaghan, J.P. (2014). The effect of local hydration environment on annular thickness and mass temporal changes. World Congress of Biomechanics, Boston, MA.

Guehring, T., et al. (2009). Notochordal intervertebral disc cells: Sensitivity to nutrient deprivation. *Arthritis and Rheumatism,* 60(4): 1026-1034.

Guehring, T., Nerlich, A., Kroeber, M., Richter, W., and Omlor, G.W. (2010). Sensitivity of notochordal disc cells to mechanical loading: An experimental animal study. *European Spine Journal,* 19: 113- 121.

Jensen, G.M. (1980). Biomechanics of the lumbar intervertebral disk: A review. *Physical Therapy,* 60: 765-773.

Johnson, W.E.B. & Roberts, S. (2003). Human intervertebral disc cell morphology and cytoskeletal composition: a preliminary study of regional variations in health and disease. *Journal of Anatomy,* 203: 605-612.

Hastreiter, D., Ozuna, R.M., and Spector, M. (2001). Regional variations in certain cellular characteristics in human lumbar intervertebral discs, including the presence of alpha-smoother muscle actin. *Journal of Orthopaedic Research*, 19(4): 597-604.

Holzapfel, G.A., Schulze-Bauer, C.A.J., and Feigl, G. (2005). Single lamellar mechanics of the human lumbar annulus fibrosus. *Biomechanical and Modeling in Biomechanics,* 3: 125-140.

Hunter, C.J., Matyas, J.R., and Duncan, N.A. (2004). The functional significance of cell clusters in the notochordal nucleus pulposus: Survival and signaling in the canine intervertebral disc. *Spine,* 29(10): 1099-1104.

Iatridis, J.C., Maclean, J.J., and Ryan, D.A. (2005). Mechanical damage to the intervertebral disc annulus fibrosus subjected to tensile loading. *Journal of Biomechanics*, 38: 557-565.

Katz, J.N. (2006). Lumbar disc disorders and low-back pain: Socioeconomic factors and consequences. *The Journal of Bone and Joint Surgery,* 88(A): 21-24.

Keller, T.S., Colloca, C.J., Harrison, D.E., Moore, R.J., and Gunzburg, R. (2007). Muscular contributions to dynamic dorsoventral lumbar spine stiffness. *European Spine Journal*, 16(2): 245-254.

Komuro, T. (1990). Re-evaluation of fibroblast and fibroblast-like cells. *Anatomy and Embryology,* 182: 103-112.

Kumar, N., Kukreti, S., Ishaque, M., Sengupta, D., and Mulholland, R.C. (2002). Functional anatomy of the deer spine: An appropriate biomechanical model for the human spine? *The Anatomical Record,* 266: 108-117.

Leung, V.Y.L., Chan, W.C.W., Hung, S-C., Cheung, K.M.C., Chan, D. (2009). Matrix remodeling during intervertebral disc growth and degeneration detected by multichromatic FAST staining. *Journal of Histochemistry and Cytochemistry*, 57(3): 249-256.

Lodish, H., Berk, A., Zipursky, S.L., Matsudaira, P., Baltimore, D., and Darnell, J. (2000). *Molecular Cell Biology (4th ed.).* New York, NY: W.H. Freeman.

Lundon, K. (2007). The effects of mechanical load on soft connective tissues. In W.I. Hammer (Ed.), *Functional Soft-Tissue Examination and Treatment by Manual Methods* (pp. 15-30). Sudbury, MA: Jones and Bartlett Publishers.

Marchand, F. and Ahmed, A.M. (1990). Investigation of the laminate structure of lumbar disc anulus fibrosus. *Spine,* 15(5): 402-410.

Maroudas, A., Stockwell, R.A., Nachemson, A., and Urban, J. (1975). Factors involved in the nutrition of the human lumbar intervertebral disc: Cellularity and diffusion of glucose *in vitro*. *Journal of Anatomy*, 120(1): 113-130.

McCann, M.R., Patel, P., Beaucage, K.L., Xiao, Y., Bacher, C., Siqueria, W.L., Holdsworth, D.W., Dixon, S.J., and Séguin, C.A. (2013). Acute vibration induces transient expression of anabolic genes in the murine intervertebral disc. *Arthritis and Rheumatism*, 65(7): 1853-1864.

McDevitt, C. A. (1988). Proteoglycans of the intervertebral disc. In P. Ghosh (Ed.), *The Biology of the Intervertebral Disc: Part I* (pp. 151-170). Boca Raton, FL: CRC Press Inc.

McGill, S. *Low Back Disorders* (2nd edition). (2007). Champaigne, Illinois: Human Kinetics Publishers.

McNally, D.S. and Adams, M.A. (1992). Internal intervertebral disc mechanics as revealed by stress profilometry. *Spine,* 17: 66-73.

Melrose, J., Smith, S., and Ghosh, P. (2003). Assessment of the cellular heterogeneity of the ovine intervertebral disc: Comparison with synovial fibroblasts and articular chondrocytes. *European Spine Journal,* 12: 57-65.

Muir, H. (1995). The chondrocyte, architect of cartilage. *BioEssays*, 17(12): 1039-1048.

Nachemson, A. (1976). The lumbar spine: An ortheopaedic challenge. *Spine,* 1(1): 59-71.

O'Connell, G.D., Vresilovic, E.J., and Elliott, D.M. (2007). Comparison of animals use in disc research to human lumbar disc geometry. *Spine*, 32(3): 328-333.

Oegema, T.R. (1993). Biochemistry of the intervertebral disc. *Clinical Sports Medicine,* 12(3): 419-439.

Ohshima, H. Tsuji, H., Hirano, N., Ishihara, H., and Yamada, H. (1989). Water diffusion pathway, swelling pressure, and biomechanical properties of the intervertebral disc during compression load. *Spine*, 14(11): 1234-1244.

Panjabi, M.M., and White, A.A. (1978). *Clinical Biomechanics of the Spine.* Philadelphia, PA: J.B. Lippincott Company.

Pflaster, D., Krag, M.H., Johnson, C.C., Haugh, L.D., and Pope, M.H. (1997). Effect of test environment on intervertebral disc hydration. *Spine*, 22(2): 133-139.

Pope, M.H., Goh, K.L., and Magnusson, M.L. (2002). Spine ergonomics. *Annual Review of Biomedical Engineering*, 4: 49-68.

Postacchini F, Bellocci M, Massobrio M. (1984). Morphologic changes in annulus fibrosus during aging: An ultrastructural study in rats. *Spine*, 9: 596–603.

Roberts, S., Urban, J.P.G., Evans, H., and Eisenstein, S.M. (1996). Transport properties of the human cartilage endplate in relation to its composition and calcification. *Spine*, 21(4): 415-420.

Roberts, S., Evans, H., Trivedi, J., and Menage, J. (2006). Histology and pathology of the human intervertebral disc. *The Journal of Bone and Joint Surgery (American Edition)*, 88-A(2): 10-14.

Roberts, S., and Urban, J.P.G. (2011). Intervertebral discs. In *Encyclopaedia of Occupational Health and Safety*. Retrieved April 1, 2013 from http://www.ilo.org/.

Rodgers, M.M., and Cavanagh, P.R. (1984). Glossary of biomechanical terms, concepts, and units. *Physical Therapy,* 64: 1886-1902..

Skrzpiec, D.M., Pollintine, P., Przbyla, A., Dolan, P., and Adamns, M.A. (2007). The internal mechanical properties of cervical intervertebral discs as revealed by stress profilometry. *European Spine Journal*, 16(10): 1701-1709.

Showalter, B.L. et al. (2012). Comparison of animal discs used in disc research to human lumbar Disc: Torsion mechanics and collagen content. *Spine*, 37(15): E900-E907.

Skaggs, D.L., Weidenbaum, M., Iatridis, J.C., Ratcliffe, A., and Mow, V.C. (1994). Regional variation in tensile properties and biochemical composition of the human lumbar anulus fibrosus. *Spine,* 19(12): 1310-1319.

Stokes, I.A.F. (1987). Surface strain on human intervertebral discs. *Journal of Orthopaedic Research,* 5: 348-355.

Sun, D.D.N., and Leong, K.W. (2004). A nonlinear hyperelastic mixture theory model for anisotropy, transport, and swelling of annulus fibrosus. *Annals of Biomedical Engineering,* 32(1): 92-102.

Sun, Y. Mauerhan, D.R., Kneisl, J.S., Norton, H.J., Zinchenko, N., Ingram, J., Hanley, E.N. Jr., and Gruber, H.E. (2012). Histological examination of collagen and proteoglycan changes in osteoarthritic menisci. *The Open Rheumatology Journal*, 6: 24-32.

Tampier, C. (2006). *Progressive Disc Herniation: An Investigation of the Mechanism Using Histochemical and Microscopic Techniques*. Ph.D. Thesis. University of Waterloo: Canada.

Tampier, C., Drake, J.D.M., Callaghan, J.P., and McGill, S.M. (2007). Progressive disc herniation: An investigation of the mechanism using radiological, histochemical, and microscopic dissection techniques on a porcine model. *Spine,* 32(25): 2869-2874.

Trout, J.J., Buckwalter, J.A., Moor, K.C., and Landas, S.K. (1982). Ultrastructure of the human intervertebral disc. 1. Changes in notochordal cells with age. *Tissue & Cell,* 14(2): 359-369.

Urban, J.P.G., Roberts, S., and Ralphs, J.R. (2000). The nucleus of the intervertebral disc from development to degeneration. *American Zoology,* 40: 53-61.

Urban, J.P.G., and Roberts, S. (2003). Degeneration of the intervertebral IVD. *Arthritis Research and Therapy,* 5(3): 120-130.

Veres, S.P, Robertson, P.A., and Broom, N.D. (2010) The influence of torsion on disc herniation when combined with flexion. *European Spine Journal*, 19: 1468-1478.

Young, O.A., and Kenrick, P.M. (1989). Muscle fibre composition of the bovine tail: A pilot study. *Anatomia, Histologia, Embryologia*, 18(1): 52-57.

Yu, J., Roberts, S., and Urban, J.P.G. (2002). Elastic fibre organization in the intervertebral discs of the bovine tail. *Journal of Anatomy,* 201: 465-475.

Yu, J. et al. (2007). Microfibrils, elastin fibres and collagen fibres in the human intervertebral disc and bovine tail disc. *Journal of Anatomy,* 210: 460-471.

Zhou, G-Q., Yang, F., Leung, V.V.L., and Cheung, K.M.C. (2008). Molecular and cellular biology of the intervertebral disc and the use of animal models. *Current Orthopaedics,* 22: 267-273.